Metal-organic Frameworks in Cooling and Water desalination: Synthesis to Application

Ramy H. Mohammed[a], Ahmed Rezk[b], Ahmed Askalany[c*], Ehab S. Ali[d], A. E. Zohir[d], Muhammad Sultan[e,f], Mohammad Ali Abdelkareem[g,h*], A.G. Olabi[g,i*]

[a]Department of Mechanical Power Engineering, Zagazig University, Egypt.
[b]Aston Institute of Materials Research, Aston University, United Kingdom.
[c]Mechanical Engineering Department, Faculty of Industrial Education, Sohag University, Egypt.
[d]Mechanical Engineering Department, Tabbin Institute for Metallurgical Studies, Egypt.
[e]Department of Agricultural Engineering, Bahauddin Zakariya University, Pakistan
[f]Adaptive AgroTech Consultancy International, USA
[g]Sustainable and Renewable Energy Engineering Department, University of Sharjah, UAE
[h]Chemical Engineering Department, Minia University. Alminya Egypt
[i]Mechanical Engineering and Design, Aston University, UK
*Corresponding: A. Askalany (ahmed_askalany3@yahoo.com), M. A. Abdelkareem (*mabulkareem@sharjah.ac.ae*), and A.G. Olabi (aolabi@sharjah.ac.ae)

Abstract

Energy-efficient alternative desalination and cooling systems are pivotal in addressing the incredible increase in ~~the~~ energy and water demands worldwide. Sorption-based technology is a unique system that could help in solving the energy and water crisis and cut down the overall carbon footprint. Such systems' performance relies on the adsorption characteristics of the employed nanoporous adsorbent. Although different nanoporous materials were developed, metal-organic frameworks (MOFs) are fast becoming a key working substance in water capture applications due to their interesting adsorption characteristics. Owing to the chemical tunability of MOFs, scientists developed thousands of MOFs in the last few decades. With the increasing interest in MOFs, this review paper provides a comprehensive survey of MOFs adsorbents and their roles in cooling and water desalination systems. Herein, three aspects are covered, the synthesis processes, the adsorption characteristics, and the implementation of MOFs at the system level. Many challenges are discussed, such as mass production, the energy demand for synthesis, and the chemical modulation of MOFs to enhance their adsorption characteristics. Many ~~types of~~ MOFs are presented, but the sorption characteristics of most of them have not been tested yet. Subsequently, a small number of the presented MOFs have been employed in sorption applications. Accordingly, a gap should be filled to test and employ the MOFs in sorption applications.

Highlights:

- Synthesis of various types of MOFs are discussed.
- Progress of MOFs adsorbents in cooling and water desalination is summarized.
- Challenges of MOF in cooling and water desalination are presented.

Keywords: Metal organic frameworks (MOFs), Adsorption desalination; Cooling, ApplicationsChallenges.

Word count: 8500

1. Introduction

Energy and water demand are experiencing a persistent rise due to the continuous population growth and socio-economic development [1, 2]. According to the EU, the energy used to cool buildings across Europe, which most of itmost of which comes from fossil fuel, is likely to increase by 72% by 2030 [3]. 40% shortfall in freshwater resources is expected by 2030 [4]. The insistent need to handle this problem has stimulated international industries and governments; for instance, the EU countries have committed to cut the greenhouse gas emissions by 40% (from 1990 levels), through increasing renewable energy in power production by 32%, and make an improvement in energy efficiency by 32.5% in 2030 [5, 6]. Although waste heat recovery resulted in improving the efficiency of the current desalination technologies [7, 8] would results in securing fresh water at lower costs with lower environmental impacts [9-11], still the usage of the renewable energy is the best choice [12, 13]. Using renewable energy resources like solar energy could alleviate the energy and water problem [14-16]. However, there is always a shift between the energy demand of the presence of the sun. So, energy conversion and management using thermally driven systems for cooling and desalination could address this problem. Among several candidates of thermally driven systems, the sorption-based system for cooling desalination (i.e., hybrid adsorption system) is a promising technology because it uses environmentally friendly working fluids, has a low maintenance cost, and could work continuously (24/7) with relatively low operating cost [17]. The sorption-based system could also be utilized for several applications like thermochemical energy storage, separation, heating, wastewater treatment, refrigeration, and desiccant air conditioning [18-21].

The characteristics of the ~~the~~ sorption-based systems depend~~s~~ mainly on the adsorbent nanoporous material employed in the system [22]. Specifically, the effectiveness of sorption cycles fundamentally depends on the ability of solid nanoporous adsorbent material to capture vapor refrigerant during a ~~certain~~ specific time [23, 24]. Therefore, high surface area per unit mass and high pore volume per unit mass of the nanoporous solid adsorbents are the main parameters that should be considered in the selection of the more suitable adsorbents for sorption technology for cooling and desalination applications. The Brunauer Emmer Teller (BET) surface area per unit mass (SSA) of commonly used adsorbents like silica gel, zeolite, and activated carbon varies from 150 m^2/g to 3100 m^2/g [25-27]. These values are still relatively small and not adequate for sorption application. So, the domain of nanoporous materials has been enlarged to develop highly porous hybrid materials. A new category of adsorbent materials with much surface area has been developed and called metal-organic frameworks (MOFs). The word MOF was first presented in 1995 by Yaghi [28], and has been used in many prospective applications, like catalysis, gas separation, gas storage, and drug delivery [29, 30]. Recently, this sort of nanoporous materials has been suggested for heat transmission systems due to its interesting microstructure [20].

Traditional adsorbents usually need either high desorption temperatures (e.g., zeolites 13X or NaA) or have unwanted linear isotherm shape (e.g., silica gel). Besides, the small surface area and pore volume of traditional adsorbents limit the performance of the adsorption cycle. MOFs are promising adsorbents for sorption cycles due to their extra-large porosity, unique adsorption properties, and tunable adsorption behavior. However, their stability and long-time synthesis process are the main challenges facing this family of nanoporous materials. In this paper, the ~~the~~ synthesis and preparation of various ~~types of~~ MOFs are reviewed and presented ~~in an appropriate wa~~appropriately. The challenges facing applying and adapting the MOFs for heat transformation applications are discussed. Also, the experimental studies that employed the MOFs for water desalination have been presented.

Commented [RA1]: Cite this paper "https://www.nature.com/articles/s41467-019-10960-0"

2. Synthesis and characteristics of MOFs

Conventional adsorbent materials "such as silica gel and zeolite" have ~~challenge~~ low capacity/update and relatively slow adsorption kinetics [17]. With excellent hydrophilicity, extra~~-~~ordinary structure, and specific host-guest interactions, MOFs seem to be the coming species of sophisticated nanoporous materials for various purposes such as thermal energy storage [31], gas storage [32, 33], cooling [34], indoor moisture control [35], and water desalination [36] [24]. The reticular synthesis method is usually applied for MOFs synthesis [37]. Secondary building units (SBUs) shown in Fig. 1 are strongly bonded to organic linkers for building up open crystalline frameworks (i.e., MOFs) with a porosity that could go up to 90% with tremendous interior specific surface area (SSA) per unit mass, as illustrated in Fig. 2. MOFs' high porosity leads to a high surface area beyond 6,000 m^2/g [38, 39]. Infinite and ordered frameworks can be formed spontaneously if ways can be suggested of connecting centers with either an octahedral or tetrahedral valence by rod-like linking units. The synthesis flexibility of MOFs has led to thousands of porous materials being constructed and reported within the last years, as shown in Fig. 3.

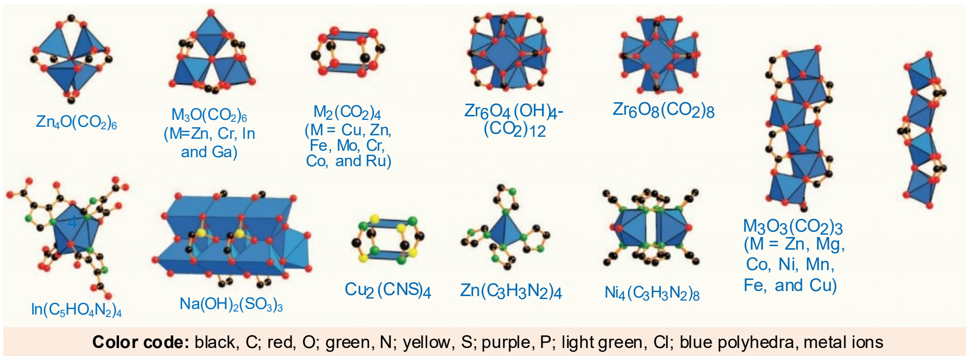

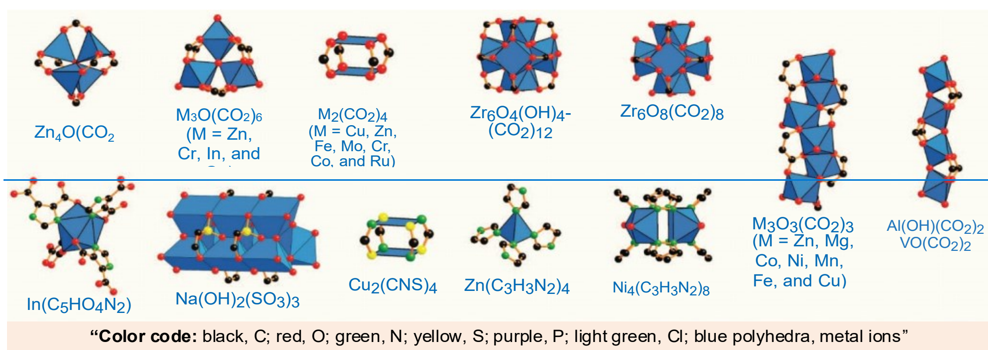

Figure 1 Inorganic secondary building units (SBUs) (Adapted from [38]*)*

Field Code Changed

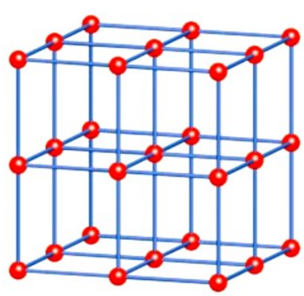

Figure 2 The topology of the MOFs structure. Color code: metal ions: red, organic linkers: blue [38].

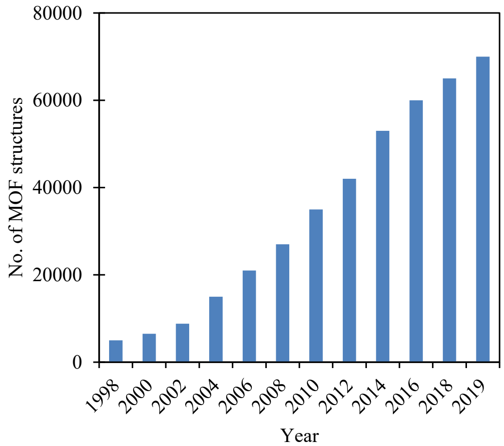

Figure 3 Reported MOFs in the Cambridge Structural Database (CSD) [40]

Abundant types of MOFs are constructed via diverse ways such as solvothermal or hydro synthesis [41], mechano-chemical synthesis [42], microwave-assisted synthesis [43], electrochemical synthesis [44], and sonochemical synthesis [45]. These methods have their own features for building up MOFs with diverse functionalization, physiochemical merits, and scale-up capability [45]. All these methods can be classified into two classes: conventional and unconventional techniques. The following section presents how MOFs are chemically formed in a comprehensive manner using different methods emphasizing with more emphasis on the conventional synthesis, which is a straightforward method of preparation of MOFs. The synthesis is generally performed by mixing salt and organic solutions at a specific temperature, following by a filtration or drying process to produce the final product [46].

2.1 Conventional methods

In the conventional method, a chemical reaction is performed using classical electric heating in the absence of parallelization of reactions. One of the main factors in MOFs synthesis is the reaction temperature. Solvothermal and non-solvothermal reactions are usually implemented. The solvothermal reaction is the reaction that occurs in a sealed chamber under pressure above the solvent boiling pressure. In turn, the non-solvothermal reaction occurs at the boiling point or below at the ambient conditions, making this method of synthesis much simple.

2.1.1 Synthesis of MOF at room temperature

MOF-2 [47], MOF-3 [48], and MOF-5 [49] were prepared by slow diffusion of TEA "organic amine trimethylamine" into metal salt. MOF-2 (Zn(BDC) (DMF) (H_2O)) can be yielded at room temperature by slow vapor diffusion of triethylamine ($N(CH_2CH_3)_3$) and toluene (C_7H_8) into DMF "dimethylformamide" solution, having a mixture of $Zn(NO_3)_2$,$6H_2O$. MOF-2 is produced as colorless prism-shaped crystals where BDC is the linkers and Zinc is the metal ions [47]. Similarly, MOF-3 ($Zn_3(BDC)_3$,$6CH_3OH$) is formed via the copolymerization method at room temperature [48]. When the *n*-propanol solution of triethylamine diffuses into the mixture (10 mL) at room temperature, the copolymerization process initiates, and block-shaped crystals form after 12 days. The crystals are gathered and washed with acetone ($(CH_3)_2CO$) and methanol (CH_3OH), and then left to dry in the air to give MOF-3 structure. MOF-5 ($Zn_4O(BDC)_3$.$(DMF)_8$) was constructed when hydrogen peroxide (with a small amount) was mixed with a mixture of triethylamine, a solution of zinc (II) nitrate, H_2BDC, DMF, and chlorobenzene (C_6H_5Cl) [49]. It was reported that the free volume of MOF-5 is about 1.04 cm^3/g. Results showed that MOF-5 has the highest porosity and the most stable one.

Huang et al. [50] synthesized two MOFs (which are called metal-organic coordination polymers (MOCPs)) using a direct mixing synthesis method at room temperature. It was reported that MOCPs are highly porous and thermally stable up to 300 ºC. MOCP-L material can be formed by directly adding pure organic amine TEA to DMF solution having $Zn(NO_3)_2.6H_2O$ and H_2BDC while a strong stirring is applied at room temperature. MOCP-L was produced whose structure is the same as MOF-5. Another MOF called MOCP-H was obtained by adding 3 drops of H_2O_2 aqueous solution to the synthesis solution. The two MOFs were found to be thermally stable. An alternative method using a room temperature synthesis was presented to prepare MOF-5, MOF-74, MOF-177, HKUST-1 (MOF-199), and IRMOF-0 [51] ambient temperature, as presented in Table 1. MOF-5 and MOF-177 were prepared using the same procedure as the following: salt and organic solutions were mixed under quick stirring, and the precipitate appeared almost instantly. The formed material was collected and evacuated overnight to vacuum pressure, then activated at a certain temperature for a specific period. Another method of producing MOF-177 at 100 ºC was proposed in Ref. [52]. A solution of DEF, H_3BTB, and $Zn(NO_3)_2$ $6H_2O$ was prepared and put in a sealed Pyrex tube that heated to 100 °C, kept for 23 h, and then cooled (12 °C/h). MOF-177 framework (block-shaped crystals) was formed, collected, and washed by DEF (4×2 ml) and finally dried in air. MOF-199 was produced by mixing organic and salt solutions. The same amount of DMF, EtOH, and H_2O were mixed to form a solvent mixture [51]. Benzene tricarboxylic acid ($C_9H_6O_6$) and $Cu(OAc)_2.H_2O$ were added separately to 12 the solvent mixture. The mixtures were mixed and stirred, and then triethylamine (Et_3N) was mixed with the reaction and stirred for almost a day. ~~Deep~~ The deep blue solid material was gathered by filtration, washed with DMF (2×25 mL), then immersed overnight in CH_2Cl_2 (50 mL). Then, the product was evacuated to less than 0.05 bar overnight, and its color turned to blue-violet. IRMOF-0 can be produced at room temperature using an organic solution of acetylene dicarboxylic acid ($C_4H_2O_4$) and DMF and salt solution of $Zn(OAc)_2.2H_2O$ [51]. After mixing the two solutions, the new solution was mixed with Triethylamine, and the reaction took place all night. Solid material was picked up by filtration and washed with 2×15 mL DMF. Then, it was evacuated overnight to 0.01 torr where IRMOF-0 was yielded.

Getachew et al. [53] presented the preparation of a MOF-2 at room temperature without using any amine. The organic linker solution was prepared by dissolving H_2BDC in DMF. The zinc salt solution was formed by dissolving Zn $(OAc)_2{\cdot}2H_2O$ in H_2O. Continuous stirring at room temperature was applied to mix the two solutions. After 15 min, a white precipitate appeared. After filtering the precipitate, it was washed repeatedly with DMF and drained off for 12h. The N_2-adsorption method reported that the SSA of MOF-2 was about 361 m^2/g.

Table 1 Synthesis of various MOFs at room temperature using salt and organic solutions

MOF	Salt solution	Organic linker solution	Processes after forming	Comments	Ref.
MOF-2	Zn $(OAc)_2 \cdot 2H_2O$ + H_2O (7.24 mmol + 0.61 mol)	H_2BDC + DMF (4.1 mmol + 0.2 mol)	Filtration, washing, drying.	- A_s was 270 m^2/g. - V_p was 0.094 cm^3/g.	[47, 54, 55]
MOF-5	$Zn(OAc)_2 \cdot 2H_2O$ + DMF (77.4 mmol + 500 mL)	$C_8H_6O_4$ + $N(CH_2CH_3)_3$ + DMF (30.5 mmol + 8.5 mL + 400 mL)	Filtration, immersing, activation, evacuation.	- Activation occurred at 120ºC for 6 h under vacuum. - 4.92 g was yielded. - A_s was found to be 3909 m^2/g.	[38, 51, 56]
MOF-74	$Zn(OAc)_2 \cdot 2H_2O$ + DEF (3.13 mmol + 20 mL)	$C_8H_6O_6$ + DMF (1.20 mmol + 20 mL)	Filtration, washing, immersing, activation, evacuation.	- 69.5 mg was yielded. - Activation occurred at 260ºC for 12 h under vacuum. - A_s was found to be 1187 m^2/g.	[51, 57, 58]
MOF-177	$Zn(OAc)_2 \cdot 2H_2O$ + DEF (11.4 mmol + 25 mL)	$C_{27}H_{18}O_6$ + DEF (1.43 mmol + 25 mL)	Filtration, washing, immersing, activation, evacuation.	- Activation occurred at 120ºC for 12 h under vacuum. - 190 g was yielded. - A_s was found to be 4944 m^2/g.	[51, 59, 60]
MOF-199	$Cu(OAc)_2 \cdot H_2O$ + DMF/H_2O/EtOH (1:1:1) (4.31 mmol + 12 mL)	$C_9H_6O_6$ + DMF/H_2O/EtOH (1:1:1) (2.38 mmol + 12 mL)	Filtration, washing, immersing, evacuation	- Activation occurred at 120ºC for 6 h under vacuum. - 316 g was yielded. - A_s was not reported.	[51, 61]
IRMOF-0	$Zn(OAc)_2 \cdot 2H_2O$ + DMF (36.4 mmol + 60 mL)	$C_4H_2O_4$ + DMF (17.6 mmol + 50 mL)	Filtration, washing, evacuation	- Activation occurred at 120ºC for 12 h under vacuum. - A_s was not reported.	[51, 62, 63]

A_s: Langmuir surface area, V_p: pore volume

2.1.2 Synthesis of MOFs by heating

MIL-100, which stands for Material of Institute Lavoisier, was synthesized as following [64]: Metallic chromium (Cr) was dissolved in 5$_M$ hydrofluoric acid, then H_2O and H_3BTC "1,3,5-benzene tricarboxylic acid" were added to the solution. In a hydrothermal unit, the mixture was heated at 20 °C/h till 220 °C, and kept at 220 °C for 96 h, and then left to cool naturally, forming a green powder. The material was collected, cleaned, and finally dried in the air, yielding MIL-100. The hydrothermal reaction was followed to prepare a highly crystallized green powder (MIL-101) using H_2BDC, $Cr(NO_3)_3.9H_2O$, fluorhydric acid, and water [65]. The reaction lasted for 8 hours at 220 °C to produce the chromium terephthalate (MIL-101). The SSA was more than 4100 m^2/g. Yang et al. [66] prepared MIL-101(Cr) (MIL-101TM) from TMAOH-$Cr(NO_3)_3$-H_2BDC-H_2O, and used it to store hydrogen. The SSA was 3197 m^2/g, and the specific pore volume was 1.73 cm^3/g. Jhung et al. [43] synthesized the porous chromium trimester (MIL-100) following the methodology presented by Ferey et al. [64], except the heating was applied using microwave irradiation. A reactant mixture was prepared using $Cr(NO_2)_3 \cdot 9H_2O$, H_2BDC (benzene dicarboxylate), HF, and H_2O with a concentration of 1:1:1:280, then put in a sealed Teflon autoclave and the temperature was increased to 210 °C. The product was collected from the solution, filtered twice, and then solvothermally treated for 20 h at 100 °C using 95% v/v ethanol. The formed material was filtered, cleaned, and finally dried in air at 150 °C. Changing the molar concentration of each component in the reaction mixture and the heating time without HF led to various versions of MIL-101 with different surface area as shown in Table 2.

Table 2 MIL-101s synthesis at 210 °C [64]

MIL-101 type	Molar composition	Heating time	SSA	V_p
A	$CrCl_3 \cdot 6H_2O$:TPA:H_2O (1:1:250)	6 h	2735	1.43
B	"$CrCl_3 \cdot 6H_2O$:TPA:H_2O (1:1:400)"	24 h	3160	1.54
C	"$CrCl_3 \cdot 6H_2O$:TPA:H_2O (1:1:550)"	24 h	ND	ND

Rowsell and Yoghi [67] supposed an alternative way to form MOF-199 ($Cu_2(C_9H_3O_6)_{4/3}$) (HKUST-1). Benzene-1,3,5-tricarboxylic acid, and Cu(II) nitrate hemi-pentahydrate were fluxed in a solution with ~~having equal concentrations of~~ DMF concentrations, ethanol, and H_2O in a bottle with stirring for 900 sec. The bottle was sealed and put in an 85 °C furnace for 20 h, where octahedral crystals were yielded afterward in a small amount. The crystals were rinsed with DMF, immersed in methanol that refilled three times in 3 days. The crystals were removed under vacuum at a temperature of 170

°C, producing MOF-199 in a porous form. IRMOF-2, IRMOF-3, IRMOF-6, IRMOF-9, IRMOF-13, and IRMOF-20 were also formed using the same strategy [67]. For instance, IRMOF-2 ($Zn_4O(C_8H_3BrO_4)_3$) was prepared by dissolving 2-Bromobenzene-1,4-dicarboxylic acid and $ZnNO_3.4H_2O$ "zinc nitrate tetrahydrate" in N,N-diethylformamide (BASF) in a glass beaker. The beaker was sealed and kept for 40 h at 100 °C to form cubic crystals. The crystals were rinsed with DMF, immersed in chloroform for 3 days, forming IRMOF-2 [67]. Other types of IRMOF were prepared by changing the reaction duration and temperature and the organic linkers presented in Table 3. IRMOF-20 has the highest SSA and specific pore volume of 3409 m^2/g and 1.53 m^3/g, respectively. However, these types of IRMOFs exhibited low stability of sorption applications. Rosi et al. [68] formed crystal structures of many new MOFs of various structure kinds used rod secondary building units. Every MOF has one of Co, Zn, Cd, Mn, Pb, or Tb, and organic linkers, as shown in Table 3. MOF-69A, B, and C were synthesized by mixing a building unit and solution of organic linkers in a vial. The mixture was then stored in a capped bottle at a specific temperature for certain days, as illustrated in Table 3.

MOF-71, MOF-72, and MOF-73 were produced by dissolving a salt solution and acid in an organic linker solution. The solid mixture was frozen using a liquid nitrogen bath to 0.2 Torr and flame-sealed. The ~~temperature of the~~ tube's temperature was increased in an iso-temperature oven and kept for a certain period, and then MOF is cooled and washed in DMF. Hexagonal plate-like crystals (MOF-71) were gathered from the oven, cleaned in DMF (3×3 mL), and air-dried. MOF-74, known as CPO-27-Zn, can be formed at 105 ºC using a mixture of H_2-DHBDC, $Zn(NO_3)_2$,4(H_2O), DMF, and water [68]. The mixture was stored and chilled in a liquid nitrogen bath to 200 mmHg. The temperature of the sealed tube was increased at a rate of 120 °C/h to 105°C for 20 h. The tube temperature was then decreased to room temperature while yellow needle crystals were formed and then air-dried. Rowsell and Yaghi supposed an alternative route to prepare MOF-74 ($Zn_2(C_8H_2O_6)$) [67]. A mixture of 2,5-Dihydroxybenzene-1,4-dicarboxylic acid, DMF, and $ZnNO_3.4H_2O$ with stirring in a 1.0 L bottle, and then deionized water was added. The tightly capped bottle was stored for 20 h in an oven at 100 ºC, where trigonal block structure was yielded afterward. The crystals were rinsed with DMF, immersed in methanol that refilled three times in 6 days. The crystals were removed under vacuum at a temperature of 270°C, producing MOF-74 in porous form.

Dietzel et al. [69] proposed another process to produce MOF-74 (CPO-27-Ni) by mixing two solutions in a Teflon-lined autoclave at 110 ºC for three days. One solution is nickel acetate tetrahydrate ($C_4H_{14}NiO_8$) and H_2O, and another mixture of 2,5-dihydroxyterephthalic acid and THF. A yellow-green fine crystalline material was gathered, filtered, and then cleaned using water. Dietzel's research team used the same process to produce CPO-27-Co and CPO-27-Zn [70]. For preparation CPO-27-Co, a solution of cobalt salt of acetic acid in water was mixed with ~~a solution of~~ H_4DOBDC and dissolved in THF. The mixture was sealed and put into 110 ºC autoclave for 72 h. Similarly, CPO-27-Zn was formed by mixing NaOH solution and $[Zn(NO_3)_2]\cdot 6H_2O$ solution in THF during stirring. At 110 ºC, the mixed solution was capped and heated up in an autoclave for three days, then a light-yellow substance (CPO-27-Zn) was gathered by filtration and washing.

MOF-75 was formed at 85 ºC as following: a solid mixture was prepared by dissolving $Tb(NO_3)_3$, $5H_2O$ and 2,5-thiophene carboxylic acid (H2-TDC) in 1 mL of DMF [68]. 1.5 mL of 2-Propanol (VC_3H_8O) was mixed with the DMF solution. The solution was cooled and vacuumed in $N_{2(l)}$ bath to 0.2 Torr and then kept to 85 °C for 15 h. The tube temperature was then reduced to room temperature to form MOF-75, which is colorless polyhedral crystals. MOF-76 was synthesized by added H_3BTC, $Tb(NO_3)_3.5H_2O$, DMF, ethanol, and H_2O to a solvothermal vessel. 2 °C/min heating rate was applied to the sealed vessel to reach 80°C for 24 h. 1 °C/min cooling rate was applied to cool down the vessel to the room temperature. Colorless crystals (MOF-76) were formed and gathered by filtration and air-dried. The same strategy was applied to form MOF-77, MOF-78, MOF-79, and MOF-80 using different solutions, as illustrated in Table 3. It is found that the preparation of these types of MOFs takes a long time and consumes more energy. MOF-75 takes about 15 h to be prepared at 85 ºC, while MOF-70 takes a week to be formed at room temperature.

Table 3 Explanation of the chemical formula of various MOFs, their Organic Carboxylates linkers, and reaction conditions

Reaction duration/temperature	Chemical formula	Organic linker	MOF type	Comment	Ref.
15h/85ºC	“$Tb(TDC)(NO_3)(DMF)_2$”	TDC	MOF-75	- 8-coordinated Tb(III) bounded by 4 carboxyl groups formed Tb-O-C rods. - It was formed as colorless polyhedral crystals.	[68]
15h/100ºC	“$Zn_3(OH)_2(1,4\text{-}BDC)_2(DEF)_2$”	1,4-BDC	MOF-69C	- It was insoluble in common organic solvents. - colorless rod-like crystals.	
15h/100ºC	“Co(1,4-BDC)(DMF)”	1,4-BDC	MOF-71	- “6-coordinated Co(II)” centres having 4 bridging carboxyl groups formed Co-O-C rods. - The MOF channels were 1.34×0.43 nm^2. - The structure was similar to that of MIL-47.	
18h/100 ºC	$Zn_4O(C_8H_5NO_4)_3$	BASF	IRMOF-3	- Solvothermal method was used. - A_s was 3062 m^2/g. - V_p was 1.07 cm^3/g.	[67]
18h/100ºC	$Zn_4O(C_{10}H_6O_4)_3$	BASF	IRMOF-6	- Solvothermal method was used. - A_s was 3263 m^2/g. - V_p was 1.14 cm^3/g.	
18h/100ºC	$Zn_4O(C_{14}H_8O_4)_3$	DMF	IRMOF-9	- Solvothermal method was used. - A_s was 2613 m^2/g. - V_p was 0.9 cm^3/g.	
18h/100ºC	$Zn_4O(C_8H_2O_4S_2)_3$	BASF	IRMOF-20	- Solvothermal method was used. - A_s was 4346 m^2/g. - V_p was 1.53 cm^3/g.	
20h/85ºC	$Cu_2(C_9H_3O_6)_{4/3}$	DMF	HKUST-1	- Solvothermal method was used. - A_s was 2175 m^2/g. - V_p was 0.75 cm^3/g.	[67]
20h/105ºC	“$Zn_2(DHBDC)(DMF)_2(H_2O)_2$”	DHBDC	MOF-74	- A_s was 245 m^2/g. - Adsorption isotherm of Type I was observed.	[68]
20h/130ºC	“$Cd_2(HPDC)_2(CHP)(H_2O)$”	HPDC	MOF-79	- “6- and 7-coordinated Cd(II)” centres built Cd-O-C rods. - It was rectangular pale-yellow crystals.	
24h/80ºC	“$Tb(BTC)(H_2O)_{1.5}(DMF)$”	BTC	MOF-76	- A_s was 334 m^2/g. - V_p 0.121 cm^3/g. - Adsorption isotherm of Type I was observed.	
24h/80ºC	“$Tb(PDC)_{1.5}(H_2O)_2(DMF)(DMF)$”	PDC	MOF-80	- It was rectangular pale-yellow crystals. - “8-coordinated Tb(III)” forming square antiprisms formed the rods. - It had channels of 1.93×0.58 nm^2.	
24h/85ºC	“$Co(HPDC)(H_2O)(DMF)_2$”	HPDC	MOF-78	- 6-coordinated Co(II) centres built Co-O-C rods. - It was rectangular pink crystals.	
40h/70ºC	$Zn_4O(C_{18}H_8O_4)_3$	DMF	IRMOF-13	- Solvothermal method was used.	

				- A_s was 2100 m^2/g. - V_p was 0.73 cm^3/g.	[67]
40h/100ºC	$Zn_4O(C_8H_3BrO_4)_3$	BASF	IRMOF-2	- Solvothermal method was used. - A_s was 2544 m^2/g. - V_p was 0.88 cm^3/g.	
40h/185ºC	$Zn_2(ATC)$	ATC	MOF-77	- tetrahedral Zn(II) centres formed Zn-O-C rods. - It was tetragonal layer rod packing. - It was stable in air and insoluble in water.	[68]
48h/100ºC	"$Mn_3(BDC)_3$ $(DEF)_2$"	1,4-BDC	MOF-73	- A_s was 181 m^2/g. - V_p was 0.061 cm^3/g. - Adsorption isotherm of Type I was observed.	
50h/140ºC	"$Cd_3(1,3\text{-}BDC)_4$ $(Me_2NH2)_2$"	1,3-BDC	MOF-72	- It was constructed from Cd-O-C rods composed of alternating 6-coordinated Cd(II) centres. - It was colorless rod-shaped crystals.	
96h/220ºC	$Cr_3F(H_2O)_3O$ $[C_6H_3\text{-}(CO_2)_3]_2$. $28H_2O$	H_3BTC	MIL-100	- Combined chemistry–simulation approach was applied. - A_s was 3100 m^2/g. - V_p was 1.16 cm^3/g.	[64]
1 week/25ºC	"$Zn_3(OH)_2$ $(BPDC)_2$ $(DEF)_4$ $(H_2O)_2$"	BPDC	MOF-69A	- It was insoluble in common organic solvents. - It was formed as colorless rod-like crystals.	[68]
1 week/25ºC	"$Zn_3(OH)_2$ $(NDC)_2$ $(DEF)_4$ $(H_2O)_2$"	NDC	MOF-69B	- It was insoluble in common organic solvents. - It was formed as colorless rod-like crystals.	
1 week/25 ºC	"$Pb(1,4\text{-}BDC)$ (C_2H_5OH) (C_2H_5OH)"	1,4-BDC	MOF-70	- 8-coordinated Pb(II) centres formed the Pb-O-C rods. - It was formed as colorless rod-like crystals. - The MOF channels were 1.31×0.54 nm^2.	

A_s: Langmuir surface area, V_p: pore volume.

Eddaoudi et al. [71] added functional groups to the phenylene links of MOF-5 (IRMOF-1) to form a new MOF. The functional groups were -Br, $-NH_2$, $-C_2H_4-$. IRMOF-2 and IRMOF-3 were prepared by dissolving acid and salt solution in organic linker solution in a glass container. The container was tightly covered, sealed, and stored in an oven for a period, and cubic crystals were yielded. The crystals were rinsed using DMF and submerged in chloroform for 3 days. After activation, porous material was prepared at room temperature under a vacuum. Later, IRMOF-3-AM1 was formed by modifying IRMOF-3 using a post-synthetic modification reaction [71]. Measurements showed that IRMOF-3-AM1 and IRMOF-3 have comparable thermal stability. The water-based green reaction process was applied to synthesize aluminum fumarate MOF [72]. $Al_2(SO_4)_3.18H_2O$ was added to water. 6.66 g was dissolved. Fumaric acid and NaOH solution were added to water while stirring in a glass beaker. A clear solution was formed by adding a droplet of a deprotonated fumaric acid solution while stirring on a hotplate at 90ºC. White produce was precipitated within 1.0 h. A centrifugal spinning machine was used to separate the product from the reaction mixture, and then it was washed and dried at 80 °C, yielding AlFum MOF. Furukawa et al. [73] prepared solvothermally many MOFs by heating solutions having zirconium salts as illustrated in Table 4.

Table 4 Preparation of different zirconium MOFs (Zr-MOF) using solvothermal method

MOF	Salt solution	Organic linker solution	Reaction temperature/Duration	Processes after forming	Comment	Ref.
MOF-801-SC	$ZrOCl_2{\cdot}8H2O$+Fumaric acid (0.23 g, 0.70 mmol)+(0.081 g, 0.70 mmol)	DMF/formic acid (35 mL/5.3 mL)	120°C/24h	1. Washing 3 times with DMF. 2. Rinsing with anhydrous DMF 3 times/day for 3 days. 3. Immersing in 0.01 L of CH_3OH for 3 days. 4. Drying under vacuum for 24 h at 150°C.	- A_s was 770 m^2/g. - V_p was 0.27 cm^3/g. - d_p was 0.56 nm.	[73, 74]
MOF-801-P (microcrystalline powder form)	$ZrOCl_2{\cdot}8H2O$+Fumaric acid (16 g, 50 mmol)+(5.8 g, 50 mmol)	DMF/formic acid (200 mL/70 mL)	130°C/6h	1. Filtering. 2. Washing 3 times with 0.02 L of fresh DMF, and another 3 times with 0.05 L of CH_3OH. 3. Rinsing with 0.05 L of DMF 3 times/day for 3 days. 4. Immersing in 0.1 L of CH_3OH for 3 days. 5. Drying at 150 °C under vacuum for 24 h.	- A_s was 1070 m^2/g. - V_p was 0.45 cm^3/g. - d_p was 0.56 nm.	[73, 75]
MOF-802	$ZrOCl_2{\cdot}8H_2O$+H_2PZDC (0.40 g, 1.3 mmol)+(0.27 g, 1.5 mmol)	DMF/formic acid (50 mL/35 mL)	130°C/72h	1. Washing 3 times with 0.005 L of DMF. 2. Rinsing with 0.01 L of DMF 3 times/day for 3 days. 3. Immersing in 0.01 L of C_3H_6O for 3 days. 4. Drying under vacuum for 24 h at 120 °C.	- A_s was < 20 m^2/g. - V_p was < 0.01 cm^3/g. - d_p was 0.56 nm.	[73, 76]
MOF-805	$ZrOCl_2{\cdot}8H_2O$+H_2NDC-$(OH)_2$ (0.032 g, 0.1 mmol)+ (0.012 g, 0.05 mmol)	DMF/formic acid (10 mL/2 mL)	120°C/24h	1. Washing 3 times with 0.003 L of DMF. 2. Rinsing with 0.005 L of DMF 3 times/day for 3 days. 3. Immersing in 0.005 L of CH_3OH for 3 days. 4. Drying under vacuum for 24 h at 120 °C.	- A_s was 1370 m^2/g. - V_p was 0.48 cm^3/g. - d_p was 0.86 nm.	[73, 77]
MOF-806	$ZrOCl_2{\cdot}8H_2O$+H_2BPDC-$(OH)_2$ (0.032 g, 0.1 mmol)+ (0.014 g, 0.05 mmol)	DMF/ formic acid (10 mL/ 2 mL)	120°C/48h	1. Washing 3 times with 0.003 L of DMF. 2. Rinsing with 0.005 L of DMF 3 times/day for 3 days. 3. Immersing in 0.005 L of C_3H_6O for 3 days. 4. Drying at 120°C under vacuum for 24h.	- A_s was 2390 m^2/g. - V_p was 0.85 cm^3/g. - d_p was 1.01 nm.	[73, 78]
MOF-808	$ZrOCl_2{\cdot}8H2O$+H_3BTC (0.16 g, 0.5 mmol)+ (0.11 g, 0.5 mmol)	DMF/ formic acid (20 mL/20 mL)	100°C/7 days	1. Washing 3 times with 0.01 L of DMF. 2. Rinsing with 0.01 L of DMF 3 times/day for 3 days. 3. Immersing in 10 mL of C_3H_6O for 3 days. 4. Drying under vacuum for 24 h at 150 °C.	- A_s was 2390 m^2/g. - V_p was 0.84 cm^3/g. - d_p was 1.84 nm.	[73, 79]
MOF-841	$ZrOCl_2{\cdot}8H2O$+H_4MTB (0.32 g, 1.0 mmol)+(0.12 g, 0.25 mmol)	DMF/ formic acid (40 mL/25 mL)	130°C/48h	1. Washing 3 times with 0.005 L of DMF. 2. Rinsing with 0.01 L of DMF 3 times/day for 3 days. 3. Immersing in 0.01 L of C_3H_6O for 3 days. 4. Drying under vacuum for 24 h at 120 °C.	- A_s was 1540 m^2/g. - V_p was 0.53 cm^3/g. - d_p was 0.92 nm.	[73, 80]
MOF-812	$ZrOCl_2{\cdot}8H2O$+H4MTB	DMF/ formic acid	130°C/24h	MOF-812 appears in low amount while preparing MOF-841.	- It was not investigated for	[73, 81]

	(0.064 g, 0.20 mmol)+ (0.048 g, 0.10 mmol)	(10 mL/6 mL)			water sorption since it was formed along with MOF-841.	
"A_s: Langmuir surface area, V_p: pore volume, d_p: pore diameter".						

Deng et al. [82] presented a general method to form crystalline MOFs. The method was based on combining groups of 2-8 links of various functional groups while the ~~ratio of the link~~link ratio was organized. First, crystals of multivariate MOFs were formed by mixing $Zn(NO_3)_2{\cdot}4H_2O$ and DMF with the acid of the chosen organic links at the conditions of MOF-5 synthesis [37,59]. Several MOFs can be synthesized using different linkers, as shown in Fig. 4. John et al. [25] applied a simple, green, and ultrafast route to prepare Zn-BDC MOF and Cu-BDC MOF at room temperature. Although the synthetic procedure was accomplished within 6 min, the BET surface area of Zn-BDC MOF and Cu-BDC MOF was very low at 4.3197 and 0.3290 m^2/g, respectively. Nasruddin et al. [83] applied the solvothermal reaction method to prepare mesoporous of Lanthanum (III)-MOF (La-NDC MOF). N_2 gas-based adsorption-desorption isotherm data was used to measure the nanostructure of the formed MOF. The SSA of La-NDC MOF was 270.38 m^2/g, and the specific pore volume was 0.16 cm^3/g. The results make this type of MOF is not suitable for cooling and desalination applications. Abedini et al. [84] synthesized Co-MOF-74 and Cu-MOF-74 using the same approaches presented in Ref. [85, 86]. Cu-MOF-74 had SSA of 1227 m^2/g and specific pore volumes of 0.69 cm^3/g. Co-MOF-74 had SSA of 1152 m^2/g and pore volume of 0.62 cm^3/g. These low values make these MOFs are not suitable for sorption-based applications. Furukawa et al. [87] proposed ultrahigh porosity MOFs using the solvothermal technique. $Zn_4O(CO_2)_6$ unit was connected with BTB, BTE, BBC, NDC, or BPDC to form MOF-177, MOF-180, MOF-205, or MOF-210, respectively. MOF-210 had the highest SSA of 6240 m^2/g and a specific pore volume of 3.6 m^3/g. Reinsch et al. [88] from Christian-Albrechts-University (CAU) prepared six MOFs, named CAU-10-X, where X could be H, CH_3, OCH_3, NO_2, NH_2, or OH. CAU-10-H had the highest SSA of 635 m^2/g, which was used later in adsorption chiller [89]. Zhou et al. [90] formed UiO-66 crystals via a two-step modulated synthesis at 120 °C. According to the amounts of acetic acid modulator added, UiO-66-0, UiO-66-1, UiO-66-2, and UiO-66-4 were prepared. UiO-66-2 exhibited the highest specific pore volume of 0.65 m^3/g and SSA of 1462 m^2/g and. Nanoporous UiO-66 was also prepared using the solvothermal method [21, 73]. Han and Chakraborty studied the adsorption characteristics UiO-66 (Zr)+water. It was found that the hydroxyl (–OH) and amino (–NH2) functional group enhances water uptake from 0.05 to 0.32 kg/kg. Compared to parent UiO-66, OH-UiO-66 could produce 10.6 m^3 more daily desalinated water per ton of adsorbent.

Commented [RA2]: Cite "https://doi.org/10.1016/j.enconman.2020.112825"

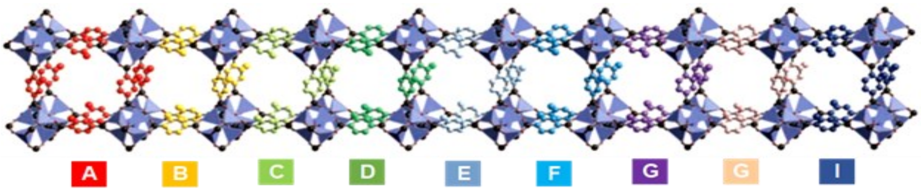

Color code: "A, 1,4-benzenedicarboxylate; B, -NH2; C, -Br; D, -(Cl)2; E, -NO2; F, -(CH3)2; G, -C4H4; H, -(OC3H5)2; and I, -(OC7H7)2"

Figure 4 General structure of various MTV-MOF-5 (Adapted from [82]*)*

2.2 Unconventional methods

The unconventional preparation of MOFs is ordinarily a mechano-chemical technique (sometimes called mechanosynthesis) where organic linker and metal salt are grinded ground in a pestle and mortar [91]. Mechanochemistry has received special interest from chemists/engineers to accelerate reactions between solids quantitatively, without either using a solvent or only little amounts [92]. Generally, three various mechanochemical ways applied for MOFs synthesis: neat grinding (NG), in which solvent is not used, LAG "liquid-assisted grinding", which is faster and more versatile, and ILAG "ion-and-liquid assisted grinding" that utilizes a catalytic liquid to promote the MOF preparation [93]. Recently, extrusion and compression way can be followed for the pilot-scale formation of MOFs [94].

HKUST-1 ($Cu_3(BTC)_2$) was prepared via NG in a shaker mill [95, 96] and via the microwave synthesis method [97]. Its SSA was measured as 1364 m^2/g when 15 min grinding time was applied [79]. The same technique was applied to form ZIF-8 (zeolitic imidazolate framework), and the SSA was 1480 m^2/g, and pore volume was 1.05 cm^3/g [98]. Paseta et al. [99] also prepared ZIF-8 using simple high-pressure synthesis. This methodology is a fast route that offers new insights into industrial implementation. Al(fumarate)(OH) was synthesized via mechanochemical method using a twin-screw extruder at 150 ºC. The MOF's SSA was 1010 m^2/g [100]. The same technique was also applied to prepare ZIF-8, HKUST-1, and MAF-4. This method was effective for covalent chemical synthesis under solvent-free. Singh et al. [101] formed MIL-78 via mechanical milling of single and mixed rare earth carbonates with TMA. Volkringer et al. [102] made MIL-100 (Al), having a BET specific surface area of 2152 m^2/g. Lenzen et al. [103] used H_2TDC as the linker to form a highly stable Al-MOF (called CAU-23). CAU-23 was formed with a high amount under green synthesis conditions. Its BET specific surface area was 1250 m^2/g, and was found to be suitable for water adsorption with an uptake of 0.37 g/g. Hu et al. [104] prepared a highly hydrophobic N-coordinated

UiO-66(Zr) via the fast mechano-chemical method. Its surface area was 1217 m^2/g, and pore volume was 0.40 cm^3/g that is similar to that prepared via a solvothermal approach [105].

Schlesinger et al. [106] prepared $Cu_3(btc)_2(H_2O)_3$ MOF using six various synthetic ways: solvothermal, atmospheric pressure and reflux, microwave-assisted, ultra-sonic, and mechanochemical conditions. The fastest way to produce $Cu_3(btc)_2(H_2O)_3$ was the microwave-assisted solvothermal synthesis. The SSA was 1499 m^2/g, and a specific pore volume was 0.79 cm^3/g. Khan and Jhung [107] used the ultrasonic irradiation method to form HKUST-1 at a reaction time of 1 min. The SSA was 1156 m^2/g, and the specific pore volume was 0.4 cm^3/g. Abbasi et al. [108] formed CuBTC MOF ($Cu_3(BTC_2)$) using either the mechanosynthesis (denoted M-CuBTC) or ultrasonic method (denoted U-CuBTC). The ultrasonic technique showed a decrease in the surface area. Ou et al. [109] synthesized PSP-MIL-53 by placing SP acrylate in the voids of MIL-53, succeeded by in situ polymerization. PSP–MOF was used for water desalination and yielded 139.51 kg/day at a low energy consumption of 0.11 Wh/L. This adsorbent showed good stability and cycling performance. Teo et al. [110] prepared Aluminium Fumarate (Al-Fum) MOF using a spinning machine. Fumaric acid and aluminum chloride hexahydrate were mixed and put into a beaker having DMF and was stirred for 96 h at 130 °C. Then, a centrifugal spinning machine was used to separate the mixture to get the Al-Fum MOF after activation at 150 ºC. The SSA was 792.26 m^2/g, and the specific pore volume was 0.926 m^3/g. Masoomi et al. [111] synthesized Cd(II) based MOF (TMU-7) by incorporation of V-shaped flexible dicarboxylate ligand and the N-donor pillar ligand using the sonochemical method. Its Bet surface area was low at 393 m^2/g, which means it is not suitable for sorption applications.

2.3 Challenges and opportunities of MOFs syntheses

Although thousands of MOFs have been prepared using different techniques, MOFs face strong challenges ~~to be able~~ to compete with conventional adsorbents similar to silica gel, activated carbons, and polymers. Most of the proposed synthesis ~~ways~~ methods have a low production rate, need critical experimental conditions, and are followed by energy-intensive post-treatments, which sometimes ~~have negative impacts on~~negatively impact the environment. Cost-efficiency is the main bottleneck, controlled by the high capital investment cost of the commercial-scale yield units. This issue could be solved by attempting to preparing MOFs using cheap synthons. Besides, the low productivity and low thermal stability of the most proposed MOFs are ~~a~~ barriers facing their implementation in commercial applications.

To raise the probability of developing ~~having~~ a stable MOF, metals ~~having~~ of higher valence such as iron (Fe), aluminum (Al), zirconium (Zr), and vanadium (V) are more recommended than metals like Zn and Cu whose valence numbers are low [112]. Using such metals can enhance the life cycle of MOFs sufficiently enough to compete with other conventional adsorbents; this directly fosters the cost efficiency of the commercialized MOF-based systems by prolonging their lifespan enough to pay back their initial investment.

Synthesize time is a critical challenge that directly impacts cost efficiency. ~~Time-consuming is also a challenge.~~ For instance, the synthesis of MOFs via hydrothermal or solvothermal methods needs many days to crystallize the material. ~~This problem could be solved using n~~Nonconventional methods ~~or~~and micro-wave irradiation are the most promising avenues to address such a challenge. They~~that has~~ have several advantages, such as rapid crystallization, narrow distributions of particulate diameter, controllable morphology, phase selectivity, and effective process parameter assessment. This approach has seldom been used for preparing inorganic-organic hybrid MOFs [*113*]. Regarding the surface area, post-synthetic modification covalently or coordinatively on MOFs is a favorable approach to introduce highly active sites [*114*].

Besides the high SSA and high pore volume, the more suitable MOFs for water sorption and heat transformation applications should also have high uptake, long thermochemical stability, relatively high thermal diffusivity, and high adsorption kinetics. All these parameters should be considered in the selection of suitable MOFs for such applications. Therefore, the most important parameters are discussed in the following sections.

~~There are s~~Several approaches were recently investigated to apply MOFs into adsorbent bed heat exchangers, such as spray coating by Kummer et al. [1], in-situ synthesis by Tan et al. [2], metal foam coating by Pinheiro et al. [3], and packing into finned heat exchanger by Saleh et al. [4]. Given the exceptional surface area of MOFs, coating and in-situ synthesis showed the best balance between the thermal and adsorption performance compared to packed beds due to minimal adsorbent/heat exchanger contact thermal resistance. Such approaches are the most promising to overcome the low thermal diffusivity of MOFs.

1. Kummer, H., et al., *A Functional Full-Scale Heat Exchanger Coated with Aluminum Fumarate Metal–Organic Framework for Adsorption Heat Transformation.* Industrial & Engineering Chemistry Research, 2017. **56**(29): p. 8393-8398.

2. Tan, B., et al., *In Situ Synthesis and Performance of Aluminum Fumarate Metal–Organic Framework Monolithic Adsorbent for Water Adsorption.* Industrial & Engineering Chemistry Research, 2019. **58**(34): p. 15712-15720.

3. Pinheiro, J.M., et al., *Copper foam coated with CPO-27(Ni) metal–organic framework for adsorption heat pump: Simulation study using OpenFOAM.* Applied Thermal Engineering, 2020. **178**: p. 115498.

3. Adsorption characteristics of the MOFs

MOF is a species of tunable adsorbents of high porosity and extra-ordinary surface area. For example, NU-110 MOF has SSA of 7140 m^2/g, which is 2.5 that of conventional adsorbents of extra-ordinary surface area (e.g., Maxsorb III). The extra-ordinary properties of MOFs make such materials encouraging candidates for various applications like desalination, separation process, and gas storage such as (e.g., hydrogen, carbon dioxide, and methane). The selection of a MOF for a certain application fundamentally depends on its pores surface area, which is directly measured by quantifying the adsorption capacity. Figure 5 shows the SSA and the corresponding pore volumes for a range of MOFs compared to conventional adsorbents. It was reported that NU-110 has the largest pore size and surface area, followed by MOF-210 and NU-100.

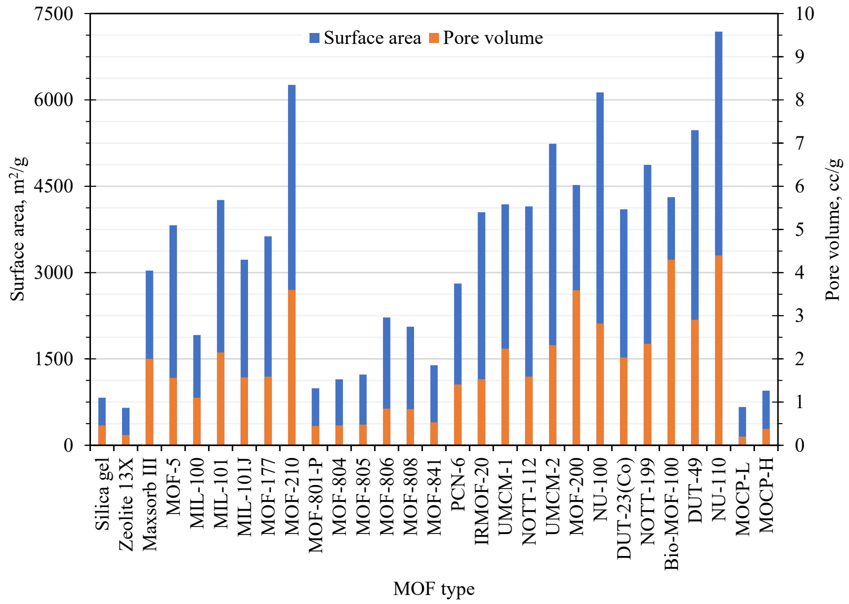

Figure 5. Specific surface area (SSA) and specific pore volume of several MOF types.

3.1 Adsorption isotherms of MOFs

Several MOF topologies have been developed, each of which shows distinctive adsorption characteristics. The developed MOF topologies may be grouped on the bases of metal ions used. The most reported metals from the material level to the device and system level are aluminum (Al), zirconium (Zr), iron (Fe), chromium (Cr), copper (Cu), magnesium (Mg), and nickel (Ni). Figure 6 presents an overview of the reported range of the maximum equilibrium uptake for seven MOF groups. Cr-MOF shows the widest range of the maximum equilibrium uptake amongst the reported MOF groups.

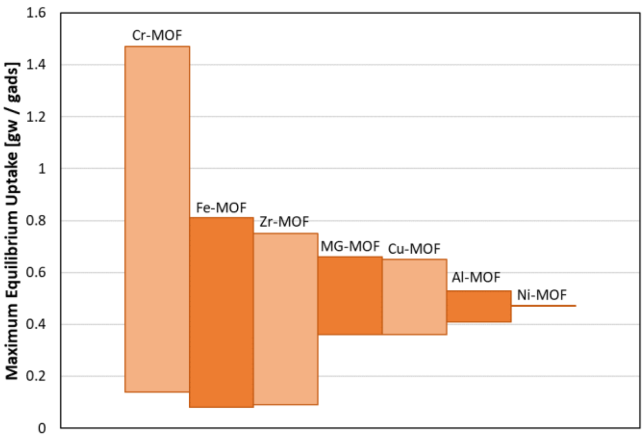

Figure 6 The range of the reported maximum equilibrium water uptake of various MOF groups [115-138].

The adsorption isotherm is a crucial characterization parameter at the material level, which governs the relationship between the adsorbate's relative pressure and its adsorption capacity. The adsorption capacity is the amount of adsorbed adsorbate taken up by the unit mass of the adsorbent. Moreover, the relative pressure in the closed-loop adsorption applications ~~is corresponding~~corresponds to the ratio between the saturation pressures of the adsorbate at the temperature of the adsorbate container to that at the temperature of the adsorbent. Traditionally, there are six types of adsorption isotherms, and each type and the maximum equilibrium uptake govern the thermodynamic cyclic performance of an adsorbent, Figure 7. The desired cyclic performance differs according to the application. For example, ~~the~~ type-I is the most preferable in adsorption cooling applications. The adsorption/desorption processes are most desirable at low relative pressure to meet the cooling temperature demand at the evaporator (adsorbate container).

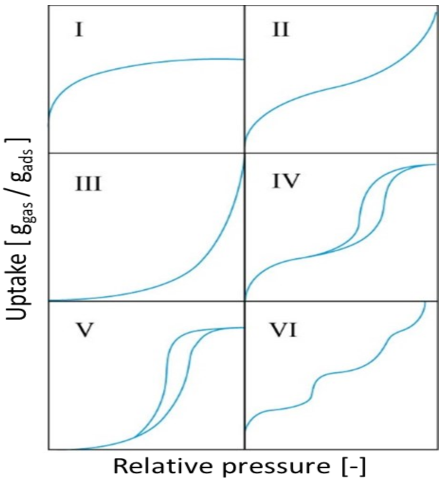

Figure 7 Types of adsorption isotherms [139]

Rezk et al. [125] [114] reported the cyclic uptake of two types of MOFs, named MIL-100 and Cu-BTC, of two different types of isotherms. For the cooling application of 5°C desired temperature in the evaporator (adsorbate container), the cyclic uptake of Cu-BTC significantly outperforms that of MIL-100; whereas, the difference of the cyclic uptake is less significant in case of the evaporator temperature increased 10°C. Owing to the stability concerns of Cu-BTC and the flexibility of the evaporation temperature in the water desalination application, MIL-100 might be more suitable as illustrated in Figure 8. Generally, most of the closed-loop water adsorption cycles concern the adsorption isotherm profile in the narrow range of partial pressure of 0.05-0.25 Pa/Pa; this is assuming the condensation and adsorption temperature are about 34°C, evaporation temperature range of 5-12°C, and desorption temperature range of 65-100°C. The evaporation temperature in the water desalination is less concerned compared to adsorption cooling and heat transformation applications. Therefore, the operating range for water desalination applications could be wider.

Figure 9 presents the water adsorption isotherms onto a selected range of MOFs, and the operating range of the closed-loop adsorption cycle; the corresponding maximum water uptakes are furnished in Table 5. The selected MOFs/water pairs were utilized in closed-loop applications such as adsorption cooling and water desalination. It is apparent from this figure that most of the reported MOFs showed S-shape (type-V) isotherm, whereas MIL-53 (Fe), Cu-BTC, CPO-27 (Ni), and Mg MOF-74 showed type-I isotherm. MIL-101 (Cr) exhibits the highest water adsorption capacity; the isotherm profile limits its application. CPO-27 Ni is the most recommended MOF because of its isotherm profile, which shows rapid uptake at low vapor pressure, good maximum equilibrium uptake, and a great deal of thermal stability. CU-BTC showed slightly higher water adsorption capacity, but its inferior uptake at low vapor pressure and stability drastically limit its application.

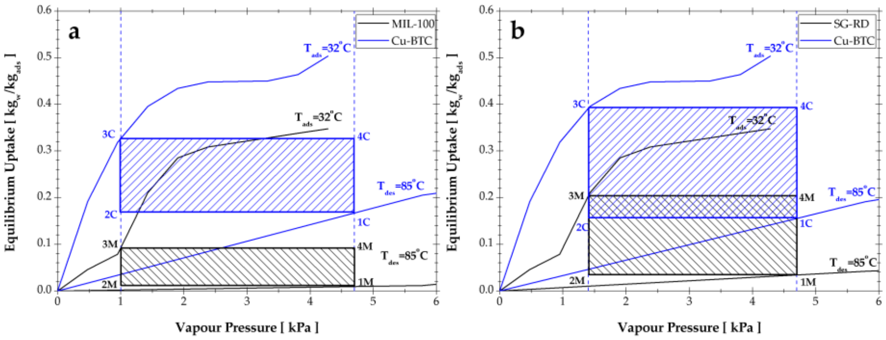

Figure 8. Comparison between two MOFs at different cyclic operating conditions [125].

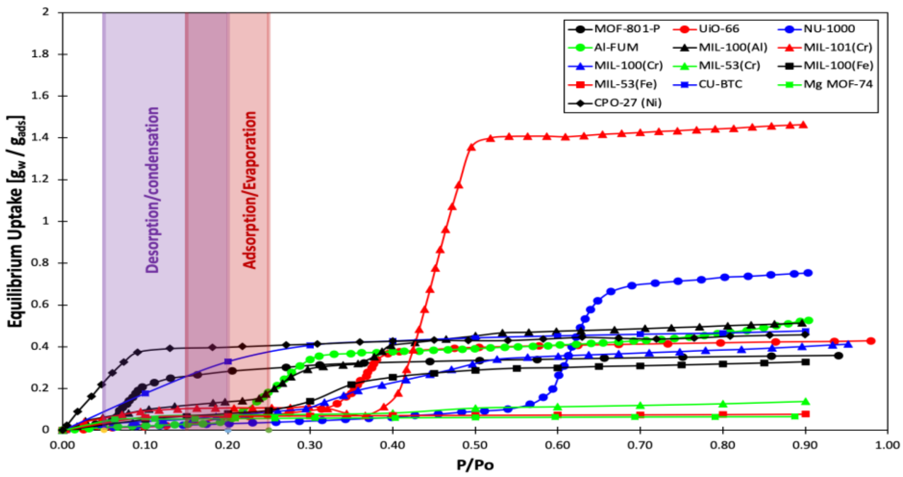

Figure 9 Adsorption isotherms of different MOF topologies

Table 5 Maximum water vapour uptake of the reported MOFs

Group	MOF	Maximum water uptake	References
Zr-MOF	MOF-801	0.4	[67, 127]
	UiO-66	0.45	[67, 127, 129] [129, 138]
	NU-1000	0.75	[67]
Al-MOF	Al-Fum	0.53	[110, 115, 118, 121]
	MIL-100(Al)	0.5	[117]

Cr-MOF	MIL-101(Cr)	1.47	[110, 115, 133, 140] [69, 116, 122, 126, 138]
	MIL-53 (Cr)	0.14	[133]
	MIL-100(Cr)	0.4	[124]
Fe-MOF	MIL-100 (Fe)	0.81	[125, 127]
	MIL-53 (Fe)	0.08	[133]
Cu-MOF	CU-BTC	0.65	[115, 125-128]
Mg-MOF	Mg-MOF-74	0.66	[128, 130]
Ni-MOF	CPO-27 Ni MOF	0.47	[121, 124, 133]

3.2 Isotherm adjustment

Generally, S-shape isotherms indicate the adsorption onto mesoporous surfaces via multilayer adsorption followed by capillary condensation. The capillary condensation phenomenon occurs below the saturation vapor pressure and restrains pores filling during the adsorption process. MOFs that show type-I isotherms might have a relatively high surface area, but the micropores accessibility is limited, and monolayer adsorption takes place. Boreskov Institute of Catalysis invented the concept of chemically embedding inorganic salt inside a hot porous structure. This concept might improve the adsorption capacity and the adsorbent isotherm of the developed composite. Building on this concept, Eman et al. [141], recently impregnated MIL-101 (Cr) with calcium chloride~~.~~.

Interestingly, the investigation showed a positive correlation between the adsorption characteristics of MIL-101 (Cr) impregnated with calcium chloride at low working relative pressure. However, the impregnation adversely impacted the BET surface area. Other phenomena need to be considered in the bulk applications at the component level, such as agglomeration and salt leakage.

4. Sorption systems of MOFs/water adsorption pairs

Adsorption cooling systems (ACS) are becoming more interested in engineering and energy research fields due to the continuous increase of space cooling and heating demands. Employment of low-grade heat sources (<150°C) from renewable energy sources like solar energy or waste heat sources from industry could reduce the consumption of fossil fuel and thus reducing the emissions of CO_2. Adsorption technologies express the utilizing of low-grade heat for generating cooling, power, and freshwater.

ACS with silica gel as adsorbent material has some drawbacks such as size, performance, and cost limitations. ~~In~~ On the contrary, MOF materials are novel porous materials with extra~~-~~ordinary adsorption capacity because of their high SSA, volume, and pore size. The main limitations of employing MOF in ACS and desalination applications are its limited hydrothermal stability and high cost. Therefore, researchers try to develop new MOF adsorption material with high hydrothermal stability and low cost. This part of the review expresses the employment of MOF materials in adsorption cooling systems and desalination.

Ehrenmann et al. [120] presented the first hydrothermal testing of adsorbent materials for utilization in thermally powered ACS. The study investigated the stability of different available adsorbent materials. A cycling test rig was performed to recognize life-cycle stress. Rezk et al. [125] expressed the adsorption features of HKUST-1 and MIL-100 MOFs experimentally. It was indicated that HKUST-1 has 93.2% higher adsorption uptake than silica gel, which could cause a rise in specific cooling power (SCP) and decreasing ACS size. Rezk et al. [125] studied adsorption properties experimentally for ethanol onto six MOF materials using DVS analyzer device. Results indicated that MIL-101Cr adsorption capacity was the highest among the tested MOFs by 1.2 kg/kg_{ads}. MIL-101Cr showed 20 successive stable cycles at 25 °C. Results showed that employing of MIL-101Cr/Ethanol pair achieved T_{evap} of -15°C with SCP of 63 W/kg. Saha et al. [142] presented experimental ethanol adsorption characteristics on MIL-101Cr for cooling applications, which were studied gravimetrically utilizing a magnetic suspension. Adsorption uptake was 1.1 $kg/kg_{ethanol}$ at 30°C. Elsayed et al. [122] investigated CPO-27(Ni) and AlFum "aluminum fumarate", which had high hydrothermal stability and water uptake of 0.47 kg/kg_{ads} and 0.53 kg/kg_{ads}, respectively. The study aimed to measure the adsorption characteristics and cyclic stability of these two MOF materials. It was indicated that the CPO-27(Ni) had better performance than the ALFum at low T_{evap} (5°C) and high T_{des} (≥ 90 °C), while the AlFum had higher suitability at T_{evap} =20°C and T_{des} =70°C.

Shi et al. [121] investigated the available CPO-27(Ni) MOF commercial feasibility for automotive ACS through theoretical modeling and experimental facility. A theoretical study of 2.4 kW two beds ACS for cars' air conditioning was investigated using the Simulink model. ~~Adsorption~~ The adsorption air conditioning system reached 440 W/ kg SCP and 0.456 COP at 130°C driving temperature, which could be provided by the exhaust gas. Automotive ACS with CPO-27(Ni) had better performance than SAPO-34 (with 42% greater in SCP), leading to a further compact system. Al-Mousawi et al. [143] studied utilizing AQSOAZ02(SAPO-34) and MIL101Cr in ACS for producing power and cooling at several operating conditions, as illustrated in Fig. 10. Results illustrated that there was potential for producing a power effect without decreasing the cooling effect. Maximum SCP was 681 $W/kg_{SAPO\text{-}34}$ and 1367 $W/kg_{MIL101Cr}$,while specific power generation (SP) was 73 $W/kg_{SAPO\text{-}34}$ and 95 $W/kg_{MIL101Cr}$.

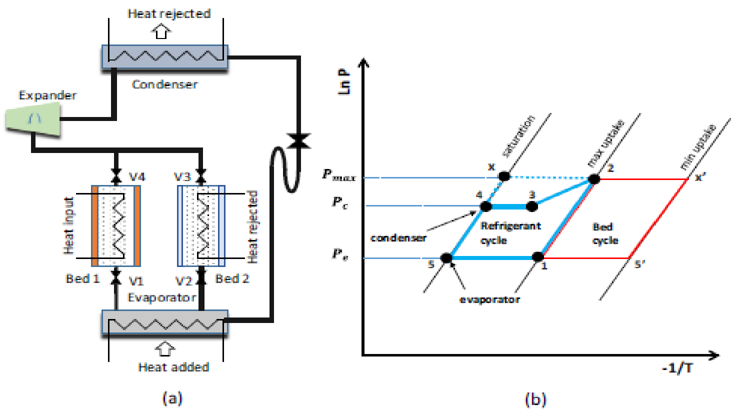

Figure 10. ACS for producing power and cooling (a) Schematic diagram. (b) Isosteric diagram [143].

Youssef et al. [144] illustrated the utilizing CPO-27(Ni) adsorbent for cooling and desalination applications experimentally, as illustrated in Fig. 11. Results illustrated that by rising evaporator temperature and decreasing condenser temperature, SCP was increased. The investigated system could produce 65 Rton/ton.ads at (T_{evap}=20 °C). SDWP was realized 22.8 m^3/ton.day at T_{evap}=40 °C,T_{con}=5°C and T_{des} = 95°C. Youssef et al. [145] investigated the ALFum theoretically for cooling/desalination applications. Figure 12 illustrates a schematic diagram of two beds ADS that had been used in this study. Results expressed that at 85°C regeneration temperature and 30°C T_{evap}, ALFum could yield 11.3 m^3/ton.day and 90.9 Rton/ ton SCP, while AQSOA-Z02 and silica-gel produced 6.4 and 8.4 m^3/ton.day and SCP of 50.5 and 62.4 Rton/ton respectively. Moreover, at low T_{des} of 65°C and T_{evap} of 10°C, ALFum yielded 3.4 m^3/ton.day and 20 Rton/ton, which were higher than AQSOA-Z02 and silica-gel.

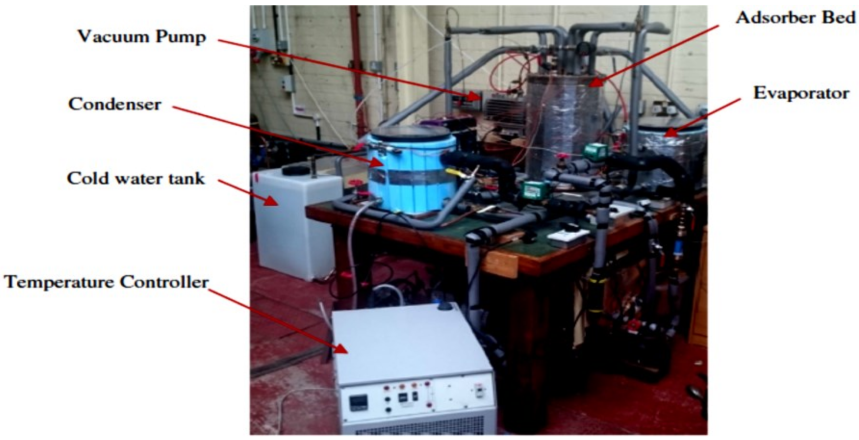

Figure 11. Pictorial view for ACS test rig [144]

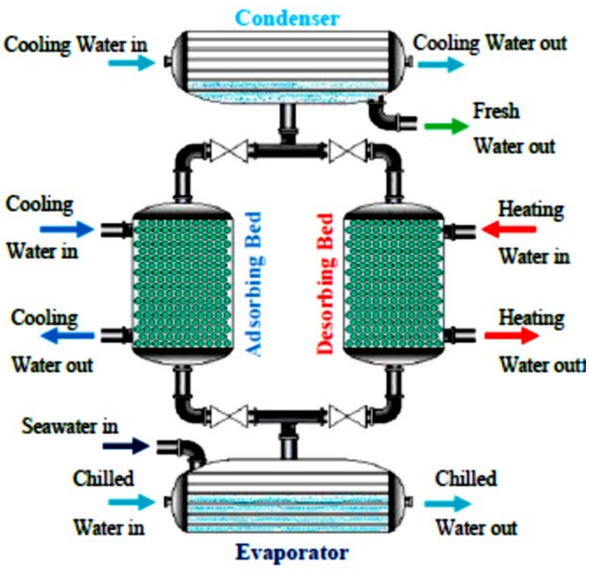

Figure 12. Schematic diagram of two-bed ADS [145]

Tatlie [146] studied ACS performance utilizing zeolite and MOF coated on a heat exchanger. The study investigated a theoretical model to estimate the best adsorbent coating thicknesses. Zeolite LiX coatings could produce higher power than zeolite NaX coatings by about 10–20%. Kummer et al. [147] presented an innovative binder-based MOF coating for ACS applications. The adsorption properties of HKUST-1/methanol and Mil-101(Cr)/methanol pairs were studied. The adsorption capacities were up to 1.22 kg/kg. Qadir et al. [148] enhanced the ACS performance utilizing an innovated "multi-walled carbon nanotube" MWCNT/MIL-100(Fe) composite adsorbent. It was obtained that innovated material could yield 455 W/kg SCP. Teo et al. [110] presented surface characteristics of alkali (Li+, Na+, K+) doped MIL-101(Cr) MOF. The adsorption properties were experimentally performed. The result obtained that proposed surface modification increased water adsorption capacity at low relative pressure. Elsayed et al. [149] investigated enhancing thermal conductivity and vapor adsorption uptake of MIL-101(Cr) utilizing hydrophilic graphene oxide (GRO). Results illustrated that adding (2%) GrO to MIL-101(Cr) increased the vapor adsorption capacity. Raising thermal conductivity was realized by adding 20-30% of GrO. Adding further 2% of GrO decreased the vapor adsorption uptake but realizing a significant increase in the thermal conductivity by around 2.5 times.

Al-Mousawi et al. [150] -used different multi-bed ACS to produce cooling and electricity. Seven Seven-beds arrangements and seven-time ratios (R) were studied employing AQSOA-Z02 and AlFum and Silica-gel. It was indicated that utilizing three-bed arrangements with R=0.5 created the best performance (SCP and SP) for ACS with utilizing silica-gel, ALFum (for T_{des} > 120 °C), and AQSOA-Z02 (for T_{des} = 160°C). Also, Using two-bed arrangements with R=1 generated the maximum COP for all adsorption materials. Dakkama et al. [151] developed MOF utilizing a nickel-based coordination polymer with open metal sites of organic frameworks for producing ice and freshwater. Figure 13 presents a schematic of the investigated system. Results showed that the optimal salinity was 35,000 ppm for highest ice production of 8.3 ton/day/ton$_{ads}$, COP was 0.9, and freshwater production was 1.8 ton/day/ton$_{ads}$.

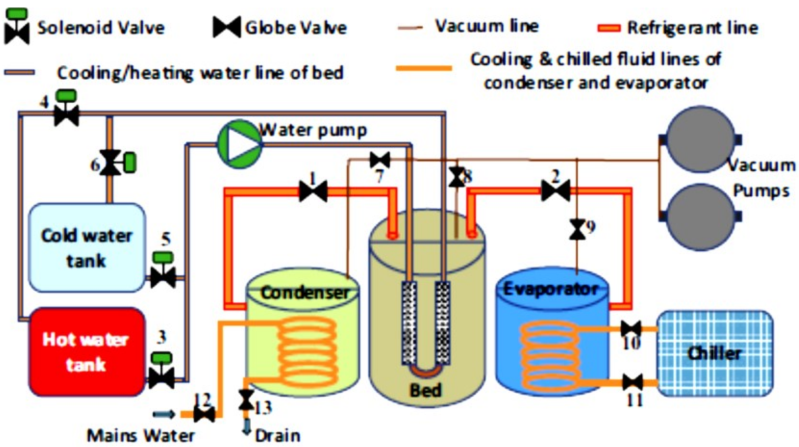

Figure 13. The schematic diagram for ice making and water desalination [151]

Elsayed et al. [116] evaluated the performance of two beds ADS by Simulink software to evaluate the utilizing of MOFs (CPO-27(Ni), MIL-101(Cr), and AlFum for AD "adsorption desalination". The result of CPO-27(Ni) showed that CPO-27(Ni) yielded about 4.3 m^3/ton/day under T_{evap} = 5 °C, while AlFum yielded about 6 m^3/ton.day under T_{evap} = 20 °C. Simultaneously, MIL-101(Cr) achieved the highest SDWP of 11 m^3/ton.day. Kayal et al. [60]reported a green technique for manufacturing AlFum. Vapor uptake on AlFum showed S-shape isotherm type with a significant increase in vapor uptake in a range of (P/Ps = 0.2–0.3), ~~which expressing efficient utilizing~~expressing efficient utilization in cooling applications. The investigated green technique for manufacturing AlFum displayed greater SCP by comparing to conventional AlFum for ACS. This technique provided a proposal for the manufacturing scale of AlFum. Teo et al. [26] developed and characterized formic acid modulated (FAM) of AlFum. An intensification in micropores distribution was detected for adding 10 ml formic acid to the AlFum. It was indicated that FAM AlFum MOFs enhanced the vapor uptake rates by 12.5% compared to the conventional AlFum for efficient utilizing in cooling applications. Qadir et al. [152] presented a new algorithm for predicting two-bed ACS performance with adjusting cycle time utilizing MIL-100(Fe). Figure 14 illustrates a schematic design of solar ACS with a two-bed configuration. The study also presented the influence of different configurations of a solar collector on the performance of ACS. Solovyeva et al. [136] expressed that at T_{ads} of 30°C, the MOF-801 could provide a cooling effect at T_{evap}= 5°C with low regenerating temperature heat (80–85°C). The SCP reached 2 kW/kg.

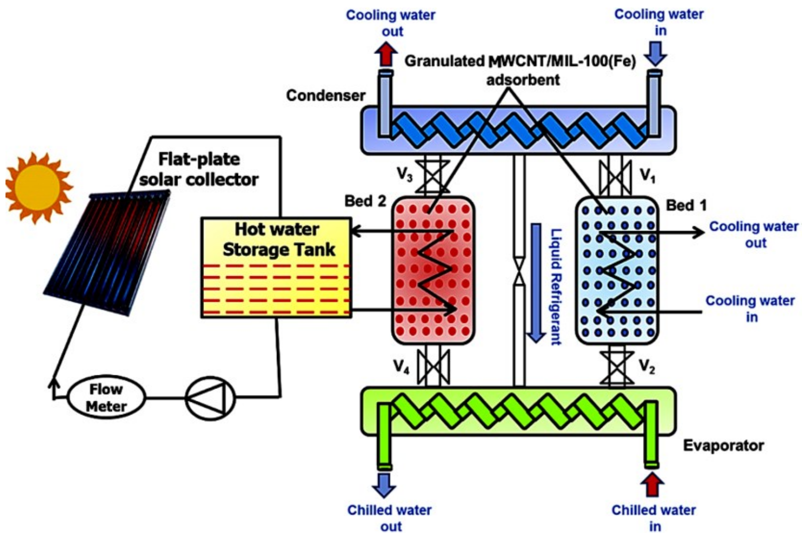

Figure 14. A schematic of the two-bed solar ACS [152].

5. Future research direction of MOFs

There are several avenues to promote the efficient utilization of MOFs in water adsorption applications to enhance the energy conversion performance at the component and system levels. A more comprehensive range of stable MOFs of S-shaped isotherms, otherwise called step-like isotherms, of high uptake at the operating partial pressure of 0.05-0.25 are needed to execute the adsorption/desorption process isothermally with the lowest possible second law deficiency [5]. They in turn, enhance the energy conversion efficiency at the system level. Although the adsorption performance of MOFs is exceptional, their thermal performance is still problematic. Therefore, it is highly advisable to use MOF as a reagent in efficient adsorption composites. Recently several graphene-based composites have been developed that showed advanced adsorbent and thermal characteristics [6]. Enhancing MOFs' thermal characteristics enhances energy conversion efficiency at the component and system level because of the intermittent operation nature of adsorption systems that require thermally agile materials to provide a fast enough thermal response. More research is required at the component level to study different practical and stable coating and in-situ synthesis of MOFs; this can significantly enhance the adsorbent/heat exchanger contact thermal resistance.

4. Saleh, M.M., et al., *Wire fin heat exchanger using aluminium fumarate for adsorption heat pumps.* Applied Thermal Engineering, 2020. **164**: p. 114426.
5. Jiang, Y., et al., *Thermodynamic limits of adsorption heat pumps: A facile method of comparing adsorption pairs.* Applied Thermal Engineering, 2019. **160**: p. 113906.
6. Rocky, K.A., et al., *Recent advances of composite adsorbents for heat transformation applications.* Thermal Science and Engineering Progress, 2021. **23**: p. 100900.

~~5.~~6. Summary

An in-depth survey about MOFs has been conducted showing synthesizing, adsorption characteristics, and sorption applications. Different ways of synthesizing have been presented, including conventional and unconventional ways such as;

- Direct coupling
- Microwave-assisted
- Microfluidic
- Spray-drying
- Microemulsion
- Electrospinning

The adsorption capacities and isotherms of different MOFs have also been presented, showing a discrepancy in the equilibrium uptake values between the different MOFs. Although MIL-101(Cr) shows the highest recorded maximum equilibrium uptake of 1.4 kg/kg, its adsorption isotherm was challenging in the cyclic operation, particularly in the adsorption cooling cycles. Building on the challenges of the adsorption characteristics of MOFs, it is essential to discuss their cyclic adsorption characteristics in the context of adsorption cooling and adsorption water desalination. Apart from the maximum equilibrium uptake, the desired cyclic operating temperature is crucial in selecting the MOF adsorbent. That led to recommending CPO-27 Ni of about 0.47 kg/kg maximum equilibrium uptake for cooling due to its excellent adsorption characteristics at low vapor pressure, achieving the desired evaporative temperature. Another promising approach of hybridizing MIL-101(Cr) with inorganic salts to modify its adsorption characteristics has been discussed. This approach might lead to better utilization of such a MOF for cooling application.

The second part introduces an overview of the adsorption capacity and isotherms of a chosen range of MOFs in water capture applications. It provides an insight into the relationship between the adsorption isotherms and their cyclic characteristics, including the potential of adjusting the adsorption isotherms to enhance their cyclic characteristics at a given range of operating temperatures. The collected data about the studied adsorption systems that are utilizing MOFs are summarized in Table 6. ~~Figure 15 also illustrates a comparison between the previous studies which investigated ACS employing MOF material as adsorbent materials.~~ Applications of MOFs in sorption cooling and/or desalination have also been included in this review showing a promising future. A SDWP value of 11.4 m^3/ton/day has been detected with a relatively low driving temperature of 85 °C. 2 kW/kg SCP has also been achieved by employing MOF-801/water.

It is clear that many MOFs have been made, but the adsorption characteristics of most of them have not been tested yet. Subsequently, a small number of the presented MOFs have been employed in sorption applications. Accordingly, the door is still open for further efforts in this area to test more of these materials and to employ them in sorption applications.

Table 6 A comparison between previous studies that investigated ACS with MOF materials.

MOF materials	**No. of bed**	**T_{cw} (°C)**	**T_{hw} (°C)**	**SDWP (m^3/ton/day)**	**SCP (W/kg)**	**COP (-)**	**Refs.**
MIL-101Cr/Ethanol	2	-	-	–	63	0.18	[135]
Aluminium Fumarate/water	–	30	85	–	–	0.4	[122]
CPO-27Ni MOF/water	–	30	85	–	–	0.67	[122]
CPO-27(Ni)/water	2	30	130	–	440	0.46	[121]
MIL101Cr/water	2	30	100	–	250	0.36	[143]

CPO-27Ni MOF/water	1	20	110	6.9	200	–	[144]
Aluminium Fumarate	2	30	85	11.3	320	0.48	[145]
MWCNT/MIL-100(Fe)	2	30	100	–	455	0.6	[148]
Aluminium Fumarate/water	2	–	100	–	320	0.54	[150]
CPO-27Ni MOF/water	1	–	95	1.8	–	0.9	[141]
CPO-27Ni MOF/water	2	25	150	4.6	134	–	[116]
Aluminium Fumarate	2	25	90	6.3	182	–	
MIL101Cr/water	2	25	150	11	315	–	
MIL- 100(Fe)	2	–	85	–	230	0.6	[142]
MOF-801/water	~~–~~2	~~29.5~~14.8	~~85~~80	–	~~2000~~540	0.~~6~~47~~7~~	[136]

Commented [RA3]: Remove this and cite "https://doi.org/10.1016/j.applthermaleng.2020.115393"

References

[1] Olabi AG, Abdelkareem MA. Energy storage systems towards 2050. Energy. 2021;219:119634.

[2] Olabi AG. Circular economy and renewable energy. Energy. 2019;181:450-4.

[3] Heating & Cooling n.d. https://www.irena.org/heatingcooling.

[4] Water Action Decade – United Nations Sustainable Development n.d. https://www.un.org/sustainabledevelopment/water-action-decade/ (accessed November 8, 2020).

[5] Chakraborty A, Ghosh S, Mukhopadhyay P, Dinara S, Bag A, Mahata M, et al. Trapping effect analysis of AlGaN/InGaN/GaN Heterostructure by conductance frequency measurement. MRS Proceedings, XXXIII. 2014;2:81-7.

[6] Commission E, Commission E. 2030 climate & energy framework. 2014.

[7] Olabi AG, Elsaid K, Rabaia MKH, Askalany AA, Abdelkareem MA. Waste heat-driven desalination systems: Perspective. Energy. 2020;209:118373.

[8] Elsaid K, Taha Sayed E, Yousef BAA, Kamal Hussien Rabaia M, Ali Abdelkareem M, Olabi AG. Recent progress on the utilization of waste heat for desalination: A review. Energy Conversion and Management. 2020;221:113105.

[9] Elsaid K, Kamil M, Sayed ET, Abdelkareem MA, Wilberforce T, Olabi A. Environmental impact of desalination technologies: A review. Science of The Total Environment. 2020;748:141528.

[10] Elsaid K, Sayed ET, Abdelkareem MA, Baroutaji A, Olabi AG. Environmental impact of desalination processes: Mitigation and control strategies. Science of The Total Environment. 2020;740:140125.

[11] Elsaid K, Sayed ET, Abdelkareem MA, Mahmoud MS, Ramadan M, Olabi AG. Environmental impact of emerging desalination technologies: A preliminary evaluation. Journal of Environmental Chemical Engineering. 2020;8:104099.

[12] Sayed ET, Wilberforce T, Elsaid K, Rabaia MKH, Abdelkareem MA, Chae K-J, et al. A critical review on Environmental Impacts of Renewable Energy Systems and Mitigation Strategies: Wind, Hydro, Biomass and Geothermal. Science of The Total Environment. 2020:144505.

[13] Rabaia MKH, Abdelkareem MA, Sayed ET, Elsaid K, Chae K-J, Wilberforce T, et al. Environmental impacts of solar energy systems: A review. Science of The Total Environment. 2021;754:141989.

[14] Abdelkareem MA, El Haj Assad M, Sayed ET, Soudan B. Recent progress in the use of renewable energy sources to power water desalination plants. Desalination. 2018;435:97-113.

[15] Rezk H, Sayed ET, Al-Dhaifallah M, Obaid M, El-Sayed AHM, Abdelkareem MA, et al. Fuel cell as an effective energy storage in reverse osmosis desalination plant powered by photovoltaic system. Energy. 2019;175:423-33.

[16] Iqbal A, Mahmoud MS, Sayed ET, Elsaid K, Abdelkareem MA, Alawadhi H, et al. Evaluation of the nanofluid-assisted desalination through solar stills in the last decade. Journal of Environmental Management. 2021;277:111415.

[17] Mohammed RH, Askalany AA. Productivity Improvements of Adsorption Desalination Systems. Solar Desalination Technology: Springer; 2019. p. 325-57.

[18] Su Y, Li Z, Zhou H, Kang S, Zhang Y, Yu C, et al. Ni/carbon aerogels derived from water induced self-assembly of Ni-MOF for adsorption and catalytic conversion of oily wastewater. Chemical Engineering Journal. 2020;402:126205.

[19] de Lange MF, Verouden KJ, Vlugt TJ, Gascon J, Kapteijn F. Adsorption-driven heat pumps: the potential of metal–organic frameworks. Chemical Reviews. 2015;115:12205-50.

[20] Karmakar A, Prabakaran V, Zhao D, Chua KJ. A review of metal-organic frameworks (MOFs) as energy-efficient desiccants for adsorption driven heat-transformation applications. Applied Energy. 2020;269:115070.

[21] Yan Z, Gong Y, Chen B, Wu X, Cui L, Xiong S, et al. Methyl functionalized Zr-Fum MOF with enhanced xenon adsorption and separation. Separation and Purification Technology. 2020;239:116514.

[22] Mohammed RH, Mesalhy O, Elsayed ML, Su M, Chow LC. Revisiting the adsorption equilibrium equations of silica-gel/water for adsorption cooling applications. International Journal of Refrigeration. 2018;86:40-7.

[23] Mohammed RH, Mesalhy O, Elsayed ML, Chow LC. Performance evaluation of a new modular packed bed for adsorption cooling systems. Applied Thermal Engineering. 2018;136:293-300.

[24] Mohammed RH, Mesalhy O, Elsayed ML, Chow LC. Novel compact bed design for adsorption cooling systems: parametric numerical study. International Journal of Refrigeration. 2017;80:238-51.

[25] El-Sharkawy II, Uddin K, Miyazaki T, Saha BB, Koyama S, Kil H-S, et al. Adsorption of ethanol onto phenol resin based adsorbents for developing next generation cooling systems. International Journal of Heat and Mass Transfer. 2015;81:171-8.

[26] Teo HWB, Chakraborty A, Han B. Water adsorption on CHA and AFI types zeolites: Modelling and investigation of adsorption chiller under static and dynamic conditions. Applied Thermal Engineering. 2017;127:35-45.

[27] Mohammed RH. Experimental and Numerical Investigation of a Novel Adsorption Bed Design for Cooling Applications. 2019.

[28] Yaghi OM, Li G, Li H. Selective binding and removal of guests in a microporous metal–organic framework. Nature. 1995;378:703-6.

[29] He H, Li R, Yang Z, Chai L, Jin L, Alhassan SI, et al. Preparation of MOFs and MOFs derived materials and their catalytic application in air pollution: A review. Catalysis Today. 2020.

[30] Ghanbari T, Abnisa F, Daud WMAW. A review on production of metal organic frameworks (MOF) for CO2 adsorption. Science of The Total Environment. 2020;707:135090.

[31] Yu S, Jing G, Li S, Li Z, Ju X. Tuning the hydrogen storage properties of MOF-650: A combined DFT and GCMC simulations study. International Journal of Hydrogen Energy. 2020;45:6757-64.

[32] Younas M, Rezakazemi M, Daud M, Wazir MB, Ahmad S, Ullah N, et al. Recent progress and remaining challenges in post-combustion CO2 capture using metal-organic frameworks (MOFs). Progress in Energy and Combustion Science. 2020;80:100849.

[33] Linxin D, Song L. Synthesis, structural characterization, methane and nitrogen adsorption of a 3D MOF {(ZnBTC)(CH3) 2NH2. DMF} n with a novel hollow-basket spheral cumulate structure. Journal of Molecular Structure.1223:128871.

[34] Han B, Chakraborty A. Adsorption characteristics of methyl-functional ligand MOF-801 and water systems: Adsorption chiller modelling and performances. Applied Thermal Engineering. 2020:115393.

[35] Ma D, Li P, Duan X, Li J, Shao P, Lang Z, et al. A Hydrolytically Stable Vanadium (IV) Metal–Organic Framework with Photocatalytic Bacteriostatic Activity for Autonomous Indoor Humidity Control. Angewandte Chemie International Edition. 2020;59:3905-9.

[36] Elsayed E, Raya A-D, Mahmoud S, Anderson P, Elsayed A. Experimental testing of aluminium fumarate MOF for adsorption desalination. Des. 2020;475:114170.

[37] John S, Mathew B, Koshy EP, George C. Green synthesis of hierarchically porous Cu-and Zn-MOFs by the combined action of hydroxy double salt and surfactant: An ultrafast method. Materials Today: Proceedings. 2020.

[38] Furukawa H, Cordova KE, O'Keeffe M, Yaghi OM. The chemistry and applications of metal-organic frameworks. Science. 2013;341.

[39] Zhou H-C, Long JR, Yaghi OM. Introduction to metal–organic frameworks. ACS Publications; 2012.

[40] The Cambridge Structural Database (CSD) - The Cambridge Crystallographic Data Centre (CCDC) n.d. https://www.ccdc.cam.ac.uk/solutions/csd-system/components/csd/ (accessed March 7, 2020).

[41] Pachfule P, Das R, Poddar P, Banerjee R. Solvothermal synthesis, structure, and properties of metal organic framework isomers derived from a partially fluorinated link. Crystal Growth & Design. 2011;11:1215-22.

[42] Klimakow M, Klobes P, Thunemann AF, Rademann K, Emmerling F. Mechanochemical synthesis of metal− organic frameworks: a fast and facile approach toward quantitative yields and high specific surface areas. Chemistry of Materials. 2010;22:5216-21.

[43] Jhung S-H, Lee J-H, Chang J-S. Microwave synthesis of a nanoporous hybrid material, chromium trimesate. Bulletin of the Korean Chemical Society. 2005;26:880-1.

[44] Martinez Joaristi A, Juan-Alcañiz J, Serra-Crespo P, Kapteijn F, Gascon J. Electrochemical synthesis of some archetypical Zn2+, Cu2+, and Al3+ metal organic frameworks. Crystal Growth & Design. 2012;12:3489-98.

[45] Haque E, Khan NA, Park JH, Jhung SH. Synthesis of a metal–organic framework material, iron terephthalate, by ultrasound, microwave, and conventional electric heating: a kinetic study. Chemistry–A European Journal. 2010;16:1046-52.

[46] Chen Z, Hanna SL, Redfern LR, Alezi D, Islamoglu T, Farha OK. Reticular chemistry in the rational synthesis of functional zirconium cluster-based MOFs. Coordination Chemistry Reviews. 2019;386:32-49.

[47] Li H, Eddaoudi M, Groy TL, Yaghi O. Establishing microporosity in open metal− organic frameworks: gas sorption isotherms for Zn (BDC)(BDC= 1, 4-benzenedicarboxylate). Journal of the American Chemical Society. 1998;120:8571-2.

[48] Li H, Davis CE, Groy TL, Kelley DG, Yaghi O. Coordinatively Unsaturated Metal Centers in the Extended Porous Framework of Zn3 (BDC) 3⊙ 6CH3OH (BDC= 1, 4-Benzenedicarboxylate). Journal of the American Chemical Society. 1998;120:2186-7.

[49] Li H, Eddaoudi M, O'Keeffe M, Yaghi OM. Design and synthesis of an exceptionally stable and highly porous metal-organic framework. nature. 1999;402:276-9.

[50] Huang L, Wang H, Chen J, Wang Z, Sun J, Zhao D, et al. Synthesis, morphology control, and properties of porous metal–organic coordination polymers. Microporous and mesoporous materials. 2003;58:105-14.

[51] Tranchemontagne DJ, Hunt JR, Yaghi OM. Room temperature synthesis of metal-organic frameworks: MOF-5, MOF-74, MOF-177, MOF-199, and IRMOF-0. Tetrahedron. 2008;64:8553-7.

[52] Chae HK, Siberio-Perez DY, Kim J, Go Y, Eddaoudi M, Matzger AJ, et al. A route to high surface area, porosity and inclusion of large molecules in crystals. Nature. 2004;427:523-7.

[53] Getachew N, Chebude Y, Diaz I, Sanchez-Sanchez M. Room temperature synthesis of metal organic framework MOF-2. Journal of Porous Materials. 2014;21:769-73.

[54] Kitagawa S, Kitaura R, Noro Si. Functional porous coordination polymers. Angewandte Chemie International Edition. 2004;43:2334-75.

[55] Zhang X, Chen Z, Liu X, Hanna SL, Wang X, Taheri-Ledari R, et al. A historical overview of the activation and porosity of metal–organic frameworks. Chemical Society Reviews. 2020;49:7406-27.

[56] Pan W, Wang J-P, Sun X-B, Wang X-X, Jiang J-y, Zhang Z-G, et al. Ultra uniform metal− organic framework-5 loading along electrospun chitosan/polyethylene oxide membrane fibers for efficient PM2. 5 removal. Journal of Cleaner Production. 2020:125270.

[57] Mancuso JL, Mroz AM, Le KN, Hendon CH. Electronic Structure Modeling of Metal–Organic Frameworks. Chemical Reviews. 2020;120:8641-715.

[58] Schnabel J, Ettlinger R, Bunzen H. Zn-MOF-74 as pH-responsive drug-delivery system of arsenic trioxide. ChemNanoMat. 2020;6:1229-36.

[59] Ryu U, Jee S, Rao PC, Shin J, Ko C, Yoon M, et al. Recent advances in process engineering and upcoming applications of metal–organic frameworks. Coordination Chemistry Reviews. 2020;426:213544.

[60] Ghazvini MF, Vahedi M, Nobar SN, Sabouri F. Investigation of the MOF Adsorbents and the Gas Adsorptive Separation Mechanisms. Journal of Environmental Chemical Engineering. 2020:104790.

[61] Xiong Z, Jiang Y, Wu Z, Yao G, Lai B. Synthesis strategies and emerging mechanisms of metal-organic frameworks for sulfate radical-based advanced oxidation process: A review. Chemical Engineering Journal. 2020:127863.

[62] Dashti A, Bahrololoomi A, Amirkhani F, Mohammadi AH. Estimation of CO2 adsorption in high capacity metal− organic frameworks: Applications to greenhouse gas control. Journal of CO2 Utilization. 2020;41:101256.

[63] Sharanyakanth P, Mahendran R. Synthesis of metal-organic frameworks (MOFs) and its application in food packaging: A critical review. Trends in Food Science & Technology. 2020.

[64] Férey G, Serre C, Mellot-Draznieks C, Millange F, Surblé S, Dutour J, et al. A hybrid solid with giant pores prepared by a combination of targeted chemistry, simulation, and powder diffraction. Angewandte Chemie. 2004;116:6456-61.

[65] Férey G, Mellot-Draznieks C, Serre C, Millange F, Dutour J, Surblé S, et al. A chromium terephthalate-based solid with unusually large pore volumes and surface area. Science. 2005;309:2040-2.

[66] Yang J, Zhao Q, Li J, Dong J. Synthesis of metal–organic framework MIL-101 in TMAOH-Cr (NO3) 3-H2BDC-H2O and its hydrogen-storage behavior. Microporous and Mesoporous Materials. 2010;130:174-9.

[67] Rowsell JL, Yaghi OM. Effects of functionalization, catenation, and variation of the metal oxide and organic linking units on the low-pressure hydrogen adsorption properties of metal− organic frameworks. Journal of the American Chemical Society. 2006;128:1304-15.

[68] Rosi NL, Kim J, Eddaoudi M, Chen B, O'Keeffe M, Yaghi OM. Rod packings and metal− organic frameworks constructed from rod-shaped secondary building units. Journal of the American Chemical Society. 2005;127:1504-18.

[69] Dietzel PD, Panella B, Hirscher M, Blom R, Fjellvåg H. Hydrogen adsorption in a nickel based coordination polymer with open metal sites in the cylindrical cavities of the desolvated framework. Chemical Communications. 2006:959-61.

[70] Dietzel PD, Johnsen RE, Blom R, Fjellvåg H. Structural changes and coordinatively unsaturated metal atoms on dehydration of honeycomb analogous microporous metal–organic frameworks. Chemistry–A European Journal. 2008;14:2389-97.

[71] Eddaoudi M, Kim J, Rosi N, Vodak D, Wachter J, O'Keeffe M, et al. Systematic design of pore size and functionality in isoreticular MOFs and their application in methane storage. Science. 2002;295:469-72.

[72] Kayal S, Chakraborty A, Teo HWB. Green synthesis and characterization of aluminium fumarate metal-organic framework for heat transformation applications. Materials Letters. 2018;221:165-7.

[73] Furukawa H, Gandara F, Zhang Y-B, Jiang J, Queen WL, Hudson MR, et al. Water adsorption in porous metal–organic frameworks and related materials. Journal of the American Chemical Society. 2014;136:4369-81.

[74] Zhang X, Wang B, Alsalme A, Xiang S, Zhang Z, Chen B. Design and applications of water-stable metal-organic frameworks: Status and challenges. Coordination Chemistry Reviews. 2020;423:213507.

[75] Chen Y, Zhang X, Mian MR, Son FA, Zhang K, Cao R, et al. Structural Diversity of Zirconium Metal–Organic Frameworks and Effect on Adsorption of Toxic Chemicals. Journal of the American Chemical Society. 2020.

[76] Feng L, Pang J, She P, Li JL, Qin JS, Du DY, et al. Metal–Organic Frameworks Based on Group 3 and 4 Metals. Advanced Materials. 2020;32:2004414.

[77] Alsadun N, Mouchaham G, Guillerm V, Czaban-Jóźwiak J, Shkurenko A, Jiang H, et al. Introducing a Cantellation Strategy for the Design of Mesoporous Zeolite-like Metal–Organic Frameworks: Zr-sod-ZMOFs as a Case Study. Journal of the American Chemical Society. 2020.

[78] Zu K, Qin M, Cui S. Progress and potential of metal-organic frameworks (MOFs) as novel desiccants for built environment control: A review. Renewable and Sustainable Energy Reviews. 2020;133:110246.

[79] Chen X, Chen D, Li N, Xu Q, Li H, He J, et al. Modified-MOF-808-Loaded Polyacrylonitrile Membrane for Highly Efficient, Simultaneous Emulsion Separation and Heavy Metal Ion Removal. ACS Applied Materials & Interfaces. 2020;12:39227-35.

[80] Hanikel N, Prévot MS, Yaghi OM. MOF water harvesters. Nature Nanotechnology. 2020:1-8.

[81] Ghasempour H, Wang K-Y, Powell JA, ZareKarizi F, Lv X-L, Morsali A, et al. Metal–organic frameworks based on multicarboxylate linkers. Coordination Chemistry Reviews. 2021;426:213542.

[82] Deng H, Doonan CJ, Furukawa H, Ferreira RB, Towne J, Knobler CB, et al. Multiple functional groups of varying ratios in metal-organic frameworks. Science. 2010;327:846-50.

[83] Zulys A, Yulia F, Buhori A, Muhadzib N, Ghiyats M, Saha BB. Synthesis and characterization of a novel microporous lanthanide based metal-organic framework (MOF) using napthalenedicarboxylate acid. Journal of Materials Research and Technology. 2020;9:7409-17.

[84] Abedini H, Shariati A, Khosravi-Nikou MR. Adsorption of propane and propylene on M-MOF-74 (M= Cu, Co): Equilibrium and kinetic study. Chemical Engineering Research and Design. 2020;153:96-106.

[85] Calleja G, Sanz R, Orcajo G, Briones D, Leo P, Martínez F. Copper-based MOF-74 material as effective acid catalyst in Friedel–Crafts acylation of anisole. Catalysis Today. 2014;227:130-7.

[86] Caskey SR, Wong-Foy AG, Matzger AJ. Dramatic tuning of carbon dioxide uptake via metal substitution in a coordination polymer with cylindrical pores. Journal of the American Chemical Society. 2008;130:10870-1.

[87] Furukawa H, Ko N, Go YB, Aratani N, Choi SB, Choi E, et al. Ultrahigh porosity in metal-organic frameworks. Science. 2010;329:424-8.

[88] Reinsch H, van der Veen MA, Gil B, Marszalek B, Verbiest T, De Vos D, et al. Structures, sorption characteristics, and nonlinear optical properties of a new series of highly stable aluminum MOFs. Chemistry of Materials. 2013;25:17-26.

[89] Lenzen D, Bendix P, Reinsch H, Fröhlich D, Kummer H, Möllers M, et al. Scalable green synthesis and full-scale test of the metal–organic framework CAU-10-H for use in adsorption-driven chillers. Advanced Materials. 2018;30:1705869.

[90] Zhou L, Zhang X, Chen Y. Modulated synthesis of zirconium metal–organic framework UiO-66 with enhanced dichloromethane adsorption capacity. Materials Letters. 2017;197:167-70.

[91] Titi HM, Do J-L, Howarth AJ, Nagapudi K, Friščić T. Simple, scalable mechanosynthesis of metal–organic frameworks using liquid-assisted resonant acoustic mixing (LA-RAM). Chemical Science. 2020.

[92] James SL, Adams CJ, Bolm C, Braga D, Collier P, Friščić T, et al. Mechanochemistry: opportunities for new and cleaner synthesis. Chemical Society Reviews. 2012;41:413-47.

[93] Beldon PJ, Fábián L, Stein RS, Thirumurugan A, Cheetham AK, Friščić T. Rapid room-temperature synthesis of zeolitic imidazolate frameworks by using mechanochemistry. Angewandte Chemie. 2010;122:9834-7.

[94] Chen D, Zhao J, Zhang P, Dai S. Mechanochemical synthesis of metal–organic frameworks. Polyhedron. 2019;162:59-64.

[95] Pichon A, Lazuen-Garay A, James SL. Solvent-free synthesis of a microporous metal–organic framework. CrystEngComm. 2006;8:211-4.

[96] Yuan W, Garay AL, Pichon A, Clowes R, Wood CD, Cooper AI, et al. Study of the mechanochemical formation and resulting properties of an archetypal MOF: Cu3 (BTC) 2 (BTC= 1, 3, 5-benzenetricarboxylate). CrystEngComm. 2010;12:4063-5.

[97] Seo Y-K, Hundal G, Jang IT, Hwang YK, Jun C-H, Chang J-S. Microwave synthesis of hybrid inorganic–organic materials including porous Cu3 (BTC) 2 from Cu (II)-trimesate mixture. Microporous and Mesoporous Materials. 2009;119:331-7.

[98] Tanaka S, Kida K, Nagaoka T, Ota T, Miyake Y. Mechanochemical dry conversion of zinc oxide to zeolitic imidazolate framework. Chemical Communications. 2013;49:7884-6.

[99] Paseta L, Potier Gg, Sorribas S, Coronas J. Solventless synthesis of MOFs at high pressure. ACS Sustainable Chemistry & Engineering. 2016;4:3780-5.

[100] Crawford D, Casaban J, Haydon R, Giri N, McNally T, James SL. Synthesis by extrusion: continuous, large-scale preparation of MOFs using little or no solvent. Chemical science. 2015;6:1645-9.

[101] Singh N, Gupta S, Pecharsky V, Balema V. Solvent-free mechanochemical synthesis and magnetic properties of rare-earth based metal-organic frameworks. Journal of Alloys and Compounds. 2017;696:118-22.

[102] Volkringer C, Popov D, Loiseau T, Férey G, Burghammer M, Riekel C, et al. Synthesis, single-crystal X-ray microdiffraction, and NMR characterizations of the giant pore metal-organic framework aluminum trimesate MIL-100. Chemistry of Materials. 2009;21:5695-7.

[103] Lenzen D, Zhao J, Ernst S-J, Wahiduzzaman M, Inge AK, Fröhlich D, et al. A metal–organic framework for efficient water-based ultra-low-temperature-driven cooling. Nature communications. 2019;10:1-9.

[104] Hu P, Liang X, Yaseen M, Sun X, Tong Z, Zhao Z, et al. Preparation of highly-hydrophobic novel N-coordinated UiO-66 (Zr) with dopamine via fast mechano-chemical method for (CHO-/Cl-)-VOCs competitive adsorption in humid environment. Chemical Engineering Journal. 2018;332:608-18.

[105] Cao Y, Zhao Y, Lv Z, Song F, Zhong Q. Preparation and enhanced CO2 adsorption capacity of UiO-66/graphene oxide composites. Journal of Industrial and Engineering Chemistry. 2015;27:102-7.

[106] Schlesinger M, Schulze S, Hietschold M, Mehring M. Evaluation of synthetic methods for microporous metal–organic frameworks exemplified by the competitive formation of [Cu2 (btc) 3 (H2O) 3] and [Cu2 (btc)(OH)(H2O)]. Microporous and Mesoporous Materials. 2010;132:121-7.

[107] Khan NA, Jhung S-H. Facile syntheses of metal-organic framework Cu 3 (BTC) 2 (H 2 O) 3 under ultrasound. Bulletin of the Korean Chemical Society. 2009;30:2921-6.

[108] Abbasi AR, Karimi M, Daasbjerg K. Efficient removal of crystal violet and methylene blue from wastewater by ultrasound nanoparticles Cu-MOF in comparison with mechanosynthesis method. Ultrasonics Sonochemistry. 2017;37:182-91.

[109] Ou R, Zhang H, Truong VX, Zhang L, Hegab HM, Han L, et al. A sunlight-responsive metal–organic framework system for sustainable water desalination. Nature Sustainability. 2020:1-7.

[110] Teo HWB, Chakraborty A, Kitagawa Y, Kayal S. Experimental study of isotherms and kinetics for adsorption of water on Aluminium Fumarate. International Journal of Heat and Mass Transfer. 2017;114:621-7.

[111] Masoomi MY, Bagheri M, Morsali A. Porosity and dye adsorption enhancement by ultrasonic synthesized Cd (II) based metal-organic framework. Ultrasonics sonochemistry. 2017;37:244-50.

[112] Wu T, Prasetya N, Li K. Recent advances in aluminium-based metal-organic frameworks (MOF) and its membrane applications. Journal of Membrane Science. 2020:118493.

[113] Jhung SH, Lee JH, Yoon JW, Serre C, Férey G, Chang JS. Microwave synthesis of chromium terephthalate MIL-101 and its benzene sorption ability. Advanced Materials. 2007;19:121-4.

[114] Lin R-B, Xiang S, Zhou W, Chen B. Microporous metal-organic framework materials for gas separation. Chem. 2020;6:337-63.

[115] Wöllner M, Klein N, Kaskel S. Measuring water adsorption processes of metal-organic frameworks for heat pump applications via optical calorimetry. Microporous and Mesoporous Materials. 2019;278:206-11.

[116] Elsayed E, Raya A-D, Mahmoud S, Anderson PA, Elsayed A, Youssef PG. CPO-27 (Ni), aluminium fumarate and MIL-101 (Cr) MOF materials for adsorption water desalination. Des. 2017;406:25-36.

[117] Jeremias F, Khutia A, Henninger SK, Janiak C. MIL-100 (Al, Fe) as water adsorbents for heat transformation purposes—a promising application. Journal of Materials Chemistry. 2012;22:10148-51.

[118] Jeremias F, Fröhlich D, Janiak C, Henninger SK. Advancement of sorption-based heat transformation by a metal coating of highly-stable, hydrophilic aluminium fumarate MOF. RSC advances. 2014;4:24073-82.

[119] Fröhlich D, Henninger SK, Janiak C. Multicycle water vapour stability of microporous breathing MOF aluminium isophthalate CAU-10-H. Dalton Transactions. 2014;43:15300-4.

[120] Ehrenmann J, Henninger SK, Janiak C. Water adsorption characteristics of MIL-101 for heat-transformation applications of MOFs. European journal of inorganic chemistry. 2011;2011:471-4.

[121] Shi B, Raya A-D, Mahmoud S, Elsayed A, Elsayed E. CPO-27 (Ni) metal–organic framework based adsorption system for automotive air conditioning. Applied Thermal Engineering. 2016;106:325-33.

[122] Elsayed E, Raya A-D, Mahmoud S, Elsayed A, Anderson PA. Aluminium fumarate and CPO-27 (Ni) MOFs: Characterization and thermodynamic analysis for adsorption heat pump applications. Applied Thermal Engineering. 2016;99:802-12.

[123] Yan J, Yu Y, Ma C, Xiao J, Xia Q, Li Y, et al. Adsorption isotherms and kinetics of water vapor on novel adsorbents MIL-101 (Cr)@ GO with super-high capacity. Applied thermal engineering. 2015;84:118-25.

[124] Wickenheisser M, Jeremias F, Henninger SK, Janiak C. Grafting of hydrophilic ethylene glycols or ethylenediamine on coordinatively unsaturated metal sites in MIL-100 (Cr) for improved water adsorption characteristics. Inorganica chimica acta. 2013;407:145-52.

[125] Rezk A, Al-Dadah R, Mahmoud S, Elsayed A. Characterisation of metal organic frameworks for adsorption cooling. International journal of heat and mass transfer. 2012;55:7366-74.

[126] Henninger S, Schmidt F, Henning H-M. Water adsorption characteristics of novel materials for heat transformation applications. Applied thermal engineering. 2010;30:1692-702.

[127] Küsgens P, Rose M, Senkovska I, Fröde H, Henschel A, Siegle S, et al. Characterization of metal-organic frameworks by water adsorption. Microporous and Mesoporous Materials. 2009;120:325-30.

[128] DeCoste JB, Peterson GW, Schindler BJ, Killops KL, Browe MA, Mahle JJ. The effect of water adsorption on the structure of the carboxylate containing metal–organic

frameworks Cu-BTC, Mg-MOF-74, and UiO-66. Journal of Materials Chemistry A. 2013;1:11922-32.

[129] Ghosh P, Colón YJ, Snurr RQ. Water adsorption in UiO-66: the importance of defects. Chemical communications. 2014;50:11329-31.

[130] Schoenecker PM, Carson CG, Jasuja H, Flemming CJ, Walton KS. Effect of water adsorption on retention of structure and surface area of metal–organic frameworks. Industrial & Engineering Chemistry Research. 2012;51:6513-9.

[131] Qiu S, Zhu G. Molecular engineering for synthesizing novel structures of metal–organic frameworks with multifunctional properties. Coordination Chemistry Reviews. 2009;253:2891-911.

[132] Henninger SK, Habib HA, Janiak C. MOFs as adsorbents for low temperature heating and cooling applications. Journal of the American Chemical Society. 2009;131:2776-7.

[133] Rezk A, Al-Dadah R, Mahmoud S, Elsayed A. Experimental investigation of metal organic frameworks characteristics for water adsorption chillers. Proceedings of the Institution of Mechanical Engineers, Part C: Journal of Mechanical Engineering Science. 2013;227:992-1005.

[134] Farha OK, Eryazici I, Jeong NC, Hauser BG, Wilmer CE, Sarjeant AA, et al. Metal–organic framework materials with ultrahigh surface areas: is the sky the limit? Journal of the American Chemical Society. 2012;134:15016-21.

[135] Rezk A, Raya A-D, Mahmoud S, Elsayed A. Investigation of Ethanol/metal organic frameworks for low temperature adsorption cooling applications. Applied energy. 2013;112:1025-31.

[136] Solovyeva M, Gordeeva L, Krieger T, Aristov YI. MOF-801 as a promising material for adsorption cooling: Equilibrium and dynamics of water adsorption. Energy conversion and management. 2018;174:356-63.

[137] Teo HWB, Chakraborty A, Kayal S. Formic acid modulated (fam) aluminium fumarate MOF for improved isotherms and kinetics with water adsorption: Cooling/heat pump applications. Microporous and Mesoporous Materials. 2018;272:109-16.

[138] Xia X, Cao M, Liu Z, Li W, Li S. Elucidation of adsorption cooling characteristics of Zr-MOFs: Effects of structure property and working fluids. Chemical Engineering Science. 2019;204:48-58.

[139] Ruthven DM. Fundamentals of adsorption equilibrium and kinetics in microporous solids. Adsorption and Diffusion: Springer; 2006. p. 1-43.

[140] Teo HWB, Chakraborty A, Kayal S. Post synthetic modification of MIL-101 (Cr) for S-shaped isotherms and fast kinetics with water adsorption. Applied Thermal Engineering. 2017;120:453-62.

[141] Elsayed E, Anderson P, Raya A-D, Mahmoud S, Elsayed A. MIL-101 (Cr)/calcium chloride composites for enhanced adsorption cooling and water desalination. Journal of Solid State Chemistry. 2019;277:123-32.

[142] Saha BB, El-Sharkawy II, Miyazaki T, Koyama S, Henninger SK, Herbst A, et al. Ethanol adsorption onto metal organic framework: Theory and experiments. Energy. 2015;79:363-70.

[143] Al-Mousawi FN, Al-Dadah R, Mahmoud S. Low grade heat driven adsorption system for cooling and power generation using advanced adsorbent materials. Energy conversion and management. 2016;126:373-84.

[144] Youssef PG, Dakkama H, Mahmoud SM, AL-Dadah RK. Experimental investigation of adsorption water desalination/cooling system using CPO-27Ni MOF. Des. 2017;404:192-9.

[145] Youssef P, Mahmoud S, Al-Dadah R, Elsayed E, El-Samni O. Numerical Investigation of Aluminum Fumarate MOF adsorbent material for adsorption desalination/cooling application. Energy Procedia. 2017;142:1693-8.

[146] Tatlier M. Performances of MOF vs. zeolite coatings in adsorption cooling applications. Applied Thermal Engineering. 2017;113:290-7.

[147] Kummer H, Baumgartner M, Hügenell P, Fröhlich D, Henninger SK, Gläser R. Thermally driven refrigeration by methanol adsorption on coatings of HKUST-1 and MIL-101 (Cr). Applied Thermal Engineering. 2017;117:689-97.

[148] ul Qadir N, Said SA, Mansour RB. Modeling the performance of a two-bed solar adsorption chiller using a multi-walled carbon nanotube/MIL-100 (Fe) composite adsorbent. Renewable Energy. 2017;109:602-12.

[149] Elsayed E, Wang H, Anderson PA, Al-Dadah R, Mahmoud S, Navarro H, et al. Development of MIL-101 (Cr)/GrO composites for adsorption heat pump applications. Microporous and Mesoporous Materials. 2017;244:180-91.

[150] Al-Mousawi FN, Al-Dadah R, Mahmoud S. Different bed configurations and time ratios: Performance analysis of low-grade heat driven adsorption system for cooling and electricity. Energy Conversion and Management. 2017;148:1028-40.

[151] Dakkama HJ, Youssef PG, Al-Dadah RK, Mahmoud S. Adsorption ice making and water desalination system using metal organic frameworks/water pair. Energy conversion and management. 2017;142:53-61.

[152] ul Qadir N, Said SA, Mansour RB. Performance prediction of a two-bed solar adsorption chiller with adaptive cycle time using a MIL-100 (Fe)/water working pair– influence of solar collector configuration. International Journal of Refrigeration. 2018;85:472-88.